Electron microscopic analysis confirmed that the produced SIVagm and SIVmnd Gag VLPs were nearly spherical, with electron-dense submembrane layers, similar to HIV-1 Gag VLPs prepared from yeast in parallel (Fig. 1C). The electron-dense submembrane layers, however, were often crescent-shaped or composed of multidomains.

Expression of HIV-2 and SIVmac Gags in yeast causes plasma membrane ruffling but no particle budding. We carried out an immunofluorescence study and examined the intracellular localization of each Gag protein. Microscopy revealed that all Gags tested (HIV-1, HIV-2, SIVmac, and SIVagm Gags) were localized predominantly in proximity to the plasma membrane (Fig. 2A). The data suggest that HIV-2 and SIVmac Gags are capable of targeting the plasma membrane in yeast, as are HIV-1 and SIVagm Gags. These findings were later confirmed by experiments in which Gags were costained with lipid rafts of the plasma membrane (Fig. 3C).

Electron microscopic analysis was carried out to examine whether Gag VLPs budded from the cell surfaces of the spheroplasts (Fig. 2B). Consistent with the results of our previous study (42), the spheroplasts expressing HIV-1 Gag showed half-spherical budding structures with electron-dense submembrane layers on the plasma membrane. A similar morphology was observed for cells expressing SIVagm Gag. In contrast, the spheroplasts expressing HIV-2 and SIVmac Gags revealed plasma membrane ruffling but no budding particle with a pinch or a thin stalk (Fig. 2B, top panels). The ruffling membrane, especially the area with outward curvature, had an electron-dense submembrane layer, suggesting that Gag proteins were gathered and budded but soon arrested at a very early stage of particle budding (Fig. 2B, top and lower middle panels). A yeast spheroplast characteristic of HIV-2 Gag expression is shown in Fig. 2B (lower middle panel). Nearly all the cells observed had plasma membrane ruffling that, in many cases, extended to a broad area of the plasma membrane. This finding was not observed for cells transformed with a parental vector (Fig. 2B, lower left panel) or for cells expressing SIVagm Gag (Fig. 2B, lower right panel).

Expression, N-terminal myristoylation, and plasma membrane targeting of HIV-2 Gag are comparable to those of HIV-1 Gag in yeast. Since HIV-2 and SIVmac fall into the same primate lentivirus lineage, HIV-2 was chosen and compared with HIV-1. We noticed that the sensitivity of the anti-HIV-2 CA antibody used was much lower than that of the anti-HIV-1 CA antibody (data not shown). For normalization, both Gag proteins were modified by adding a Flag epitope tag at the C terminus and were detected by an anti-Flag antibody. Expression of the Gags in yeast and VLP production were carried out as described above. Western blotting using anti-Flag antibody confirmed that no Gag VLP production was observed for HIV-2 Gag, despite the nearly equivalent levels of Gag expression in the cells (Fig. 3A). These data indicate that yeast essentially does not support HIV-2 Gag VLP production.

Because the failure was not due to a low level of HIV-2 Gag expression in yeast, we next examined the levels of Gag N-terminal myristoylation. Yeast cells were metabolically labeled with [9,10(n)-^{3}H]myristic acid and subjected to SDS-PAGE followed by fluorography. In both cases, one major radiolabeled band was detected at a gel position identical to that of the band detected by Western blotting probed with anti-CA antibody. The data clearly showed that the efficiencies of ^{3}H incorporation were comparable between the two Gags, indicating that both Gags were equally myristoylated in yeast (Fig. 3B). A protein myristoylation signal lies on the eight N-terminal amino acid residues (51), and the N-terminal amino acid sequences are well conserved between HIV-1 and HIV-2 Gags (Fig. 3B).

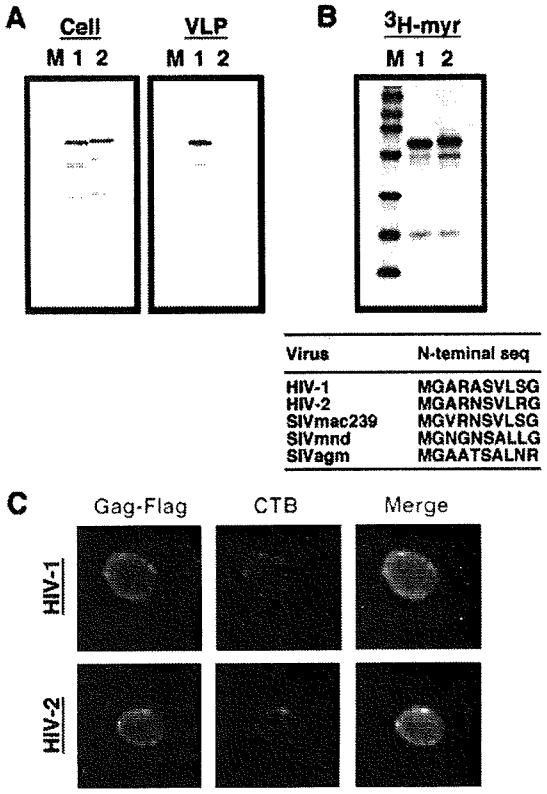

FIG. 3. N-terminal myristoylation, plasma membrane targeting, and VLP production of HIV-1 and HIV-2 Gags. Yeast cells were transformed with a pKT10 vector containing the HIV-1 or HIV-2 *gag* gene with a Flag epitope sequence added at the C terminus. (A) Intracellular Gag expression and Gag VLP production. Preparation of samples was carried out as described in the legend for Fig. 1. SDS-PAGE was followed by Western blotting using anti-Flag antibody. Lanes: M, prestained molecular weight markers; 1 and 2, expression of HIV-1 and HIV-2 Gag-Flag, respectively. (B) N-terminal myristoylation of Gag. HIV-1 and HIV-2 Gag-Flag proteins were metabolically labeled with [^{3}H]myristic acid in yeast and subjected to SDS-PAGE. Lanes: M, ^{14}C-labeled molecular weight markers; 1 and 2, cells expressing HIV-1 and HIV-2 Gag-Flag, respectively. (C) Intracellular distribution of Gag. Yeast spheroplasts expressing HIV-1 and HIV-2 Gag-Flag were incubated with CTB and then anti-CTB antibody at 4°C (not to allow endocytosis) (shown in red). After fixation with 3.7% formalin, the spheroplasts were permeabilized with 0.1% Triton X-100 and costained with anti-Flag antibody (shown in green).

We observed that both Gags similarly localized in proximity to the plasma membrane (Fig. 2A). To confirm the plasma membrane targeting, lipid rafts of the yeast plasma membrane were probed with CTB and Gag-Flag was costained with anti-Flag antibody, as recent studies have identified the presence of lipid rafts in the yeast membrane (1). Microscopy revealed that HIV-1 Gag-Flag localized on the cell periphery, with partial colocalization with lipid rafts on the plasma membrane. Similar

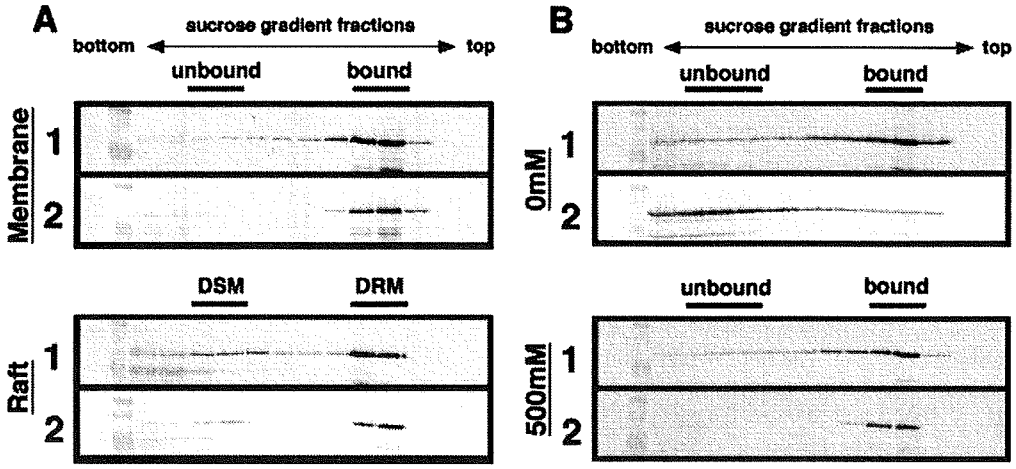

FIG. 4. Membrane and lipid raft associations of HIV-1 and HIV-2 Gags in yeast. Protein expression in yeast was carried out as described in the legend for Fig. 3. Panels: 1, cells expressing HIV-1 Gag-Flag; 2, cells expressing HIV-2 Gag-Flag. (A) Membrane and lipid raft associations of Gags at a physiological concentration of salt. Following formation of spheroplasts, cells (10 OD units) were resuspended in buffer with 150 mM NaCl and disrupted by sonication. For analysis of lipid raft association, the cell lysate was treated on ice with 0.5% Triton X-100 for 10 min. The cell lysate was clarified by low-speed centrifugation and subjected to equilibrium flotation centrifugation using a 70%-65%-10% (wt/vol) sucrose step gradient. The gradient fractions were collected from the bottom to the top (left to right) and analyzed by Western blotting using anti-Flag antibody. DSM, detergent-sensitive membrane; DRM, detergent-resistant membrane. (B) Membrane affinity of Gag in the absence of salt or under high-salt conditions. Spheroplasts (10 OD units) were resuspended in buffer, with or without 500 mM NaCl, and disrupted by sonication. After clarification by brief centrifugation, the cell lysate was subjected to equilibrium flotation centrifugation as described above.

findings were observed for HIV-2 Gag-Flag, indicating that both Gags were capable of being targeted to the plasma membrane in yeast (Fig. 3C).

HIV-2 Gag dissociates from yeast membrane in the absence of salt. To test the membrane-binding ability of Gag, membrane flotation experiments were carried out using sucrose step gradients. The initial analysis was performed at a physiological concentration of salt (150 mM NaCl). When cells expressing HIV-1 Gag-Flag were analyzed, Gag was detected in the interface fractions between the 10% and 65% sucrose layers. A similar flotation profile was observed for HIV-2 Gag-Flag, indicating that both Gags efficiently bound to the yeast membrane (Fig. 4A, top panels). It has been shown that lipid rafts are membrane microdomains that are insoluble by nonionic detergents and function as a platform for particle assembly and budding (29, 33). A similar detergent insensitivity has been reported for lipid rafts of yeast (1). Thus, Gag association with yeast lipid rafts was examined by similar equilibrium flotation centrifugation, but after a 0.5% Triton X-100 treatment on ice. When cells expressing HIV-1 Gag-Flag were analyzed, the majority of Gag was distributed in the detergent-resistant membrane fractions, suggesting that a relatively large population of the membrane-bound Gag was incorporated into the raft fractions. Very similar findings were observed for HIV-2 Gag-Flag (Fig. 4A, bottom panels). These data indicate that the two Gags show equal membrane-binding abilities and incorporation into lipid raft fractions in yeast.

However, when the sample preparation was carried out in the absence of salt and subjected to membrane flotation analysis, a striking difference was observed between the behaviors of HIV-1 and HIV-2 Gags: HIV-1 Gag displayed membrane binding, but HIV-2 Gag did not (Fig. 4B, top panels). In contrast, no differences were observed when the samples were prepared under high-salt conditions (Fig. 4B, bottom panels). These results suggest that although both Gags bind efficiently to the yeast membrane, HIV-2 Gag more readily dissociates in the absence of salt than does HIV-1 Gag.

HIV-2 Gag fails to form high-order multimers in yeast. The Gag distribution in yeast was also examined by subcellular fractionation experiments. A differential sedimentation procedure (13) yielded P13, P100, and S100 fractions, and the fractions were probed for organelle markers by Western blotting. Consistent with previous reports (13), alkaline phosphatase (for vacuoles) was found in the P13 fraction, while Pep12 (for endosomes) was found predominantly in the P100 fraction. Phosphoglycerate kinase is an abundant cytosolic protein and therefore was localized to the S100 fraction. The CTB bound to lipid rafts of the spheroplast surfaces was found in the P13 fraction (Fig. 5A, left panel). When fractions were prepared at a physiological concentration of salt (150 mM NaCl) and subjected to Western blotting, for both Gags the majority of Gag was observed in the P13 and P100 fractions, indicating that HIV-2 Gag similarly associated with the yeast membrane. However, when the fractionation was carried out in the absence of salt, the Gag distributions differed. The HIV-2 Gag shifted predominantly to the S100 fraction, while in contrast, HIV-1 Gag was detected in the same fractions as those observed in the presence of salt, confirming that HIV-2 Gag easily dissociated from the yeast membrane in the presence of salt (Fig. 5A, right panel).

To further understand these phenomena, the subcellular fractions were subjected to sedimentation analysis on 20 to 70% sucrose gradients and Gag antigens spread within the gradients were detected by Western blotting (Fig. 5B). The initial analysis was performed using the samples prepared in the absence of salt (Fig. 5B, right panels). When the whole-cell lysate from yeast expressing HIV-1 Gag was analyzed, Gag antigens were found in the 25 to 30% and 50% sucrose frac-

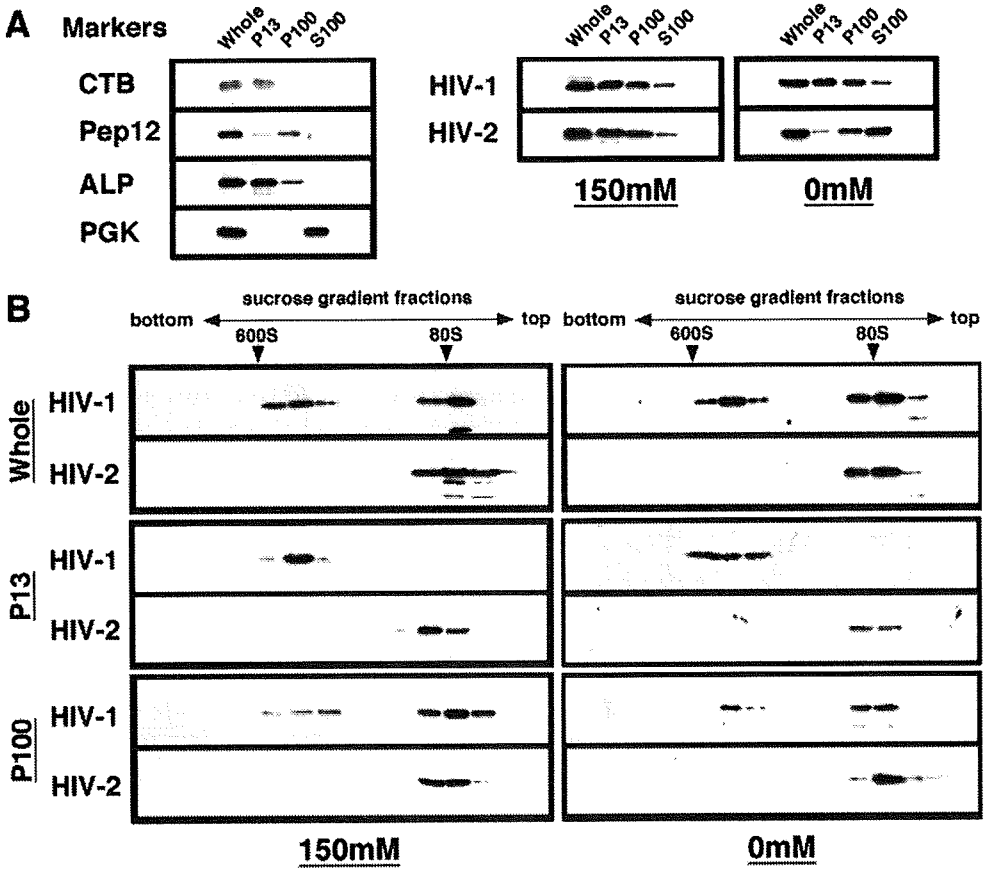

FIG. 5. Subcellular fractionation of yeast and sedimentation analysis of HIV-1 and HIV-2 Gags. Protein expression in yeast was carried out as described in the legend for Fig. 3. Following the formation of spheroplasts, cells (10 OD units) were resuspended in buffer with or without salt. (A) Subcellular fractionation. Subcellular fractionation was carried out in the presence or absence of salt, and Gag distribution was monitored by Western blotting using anti-Flag antibody (right panels). Subcellular fractions were probed for the following organelle markers: CTB (for lipid rafts on the plasma membrane), Pep12 (for endosomes), alkaline phosphatase (ALP) (for vacuoles), and phosphoglycerate kinase (PGK) (for cytosol) (left panel). (B) Sedimentation analysis of Gag. The whole-cell lysate and subcellular fractions were analyzed on 20 to 70% sucrose gradients by centrifugation at 120,000 × *g* for 2 h, and gradient fractions were subjected to Western blotting using anti-Flag antibody. Arrowheads show sedimented positions of the immature form of HIV capsid (600S) and of 80S ribosomes.

tions, likely corresponding to relatively small- and large-molecular-weight complexes, respectively. In contrast, sedimentation analysis using the whole-cell lysate from yeast expressing HIV-2 Gag revealed the presence of a Gag complex in the 25 to 30% sucrose fractions, but no other larger classes of Gag complex were seen. For more physiological conditions, we prepared the whole-cell lysate in the presence of 150 mM NaCl and carried out sedimentation analysis (Fig. 5B, left panels). The sedimentation profiles were essentially similar to those of the samples prepared in the absence of salt. These data indicate that HIV-2 Gag does not form high-order Gag multimers in yeast, although it cannot be ruled out that sedimentation analysis through 20 to 70% sucrose gradients might lead to dissociation of high-order assembly of HIV-2 Gag. The P13 and P100 fractions were also subjected to sedimentation analysis. In the case of HIV-1 Gag, the P13 fractions included predominantly the higher-order Gag multimers, while the P100 fractions included both high- and low-order Gag multimers, suggesting, though not proving, higher-order Gag assembly at the plasma membrane rather than at the endosome fractions. As expected, no high-order HIV-2 Gag multimers were detected in the P13 or P100 fraction.

Both HIV-1 and HIV-2 Gags efficiently associate with the mammalian cell membrane and form high-order multimers. For comparison, we expressed HIV-1 and HIV-2 Gag-Flag in higher eukaryotic cells, such as HeLa and 293T cells. Intracellular expression and particle production were examined by Western blotting using anti-Flag antibody. The expression levels in the cells were broadly comparable, and the production of HIV-2 particles was not impaired in either HeLa or 293T cells (Fig. 6A). Consistent with these results, when the membrane-binding affinities of Gags in the absence of salt were analyzed by membrane flotation centrifugation, the majority of Gag was found in membrane-bound fractions for both Gag types (Fig. 6B). Furthermore, when the whole-cell lysate was prepared in the absence of salt and subjected to sedimentation analysis on 20 to 70% sucrose gradients, high-order Gag multimers which sedimented in the 50% sucrose fractions were observed for both Gag types (Fig. 6C). Together, these results indicate that HIV-2 Gag, similar to HIV-1 Gag, bound efficiently to the cell

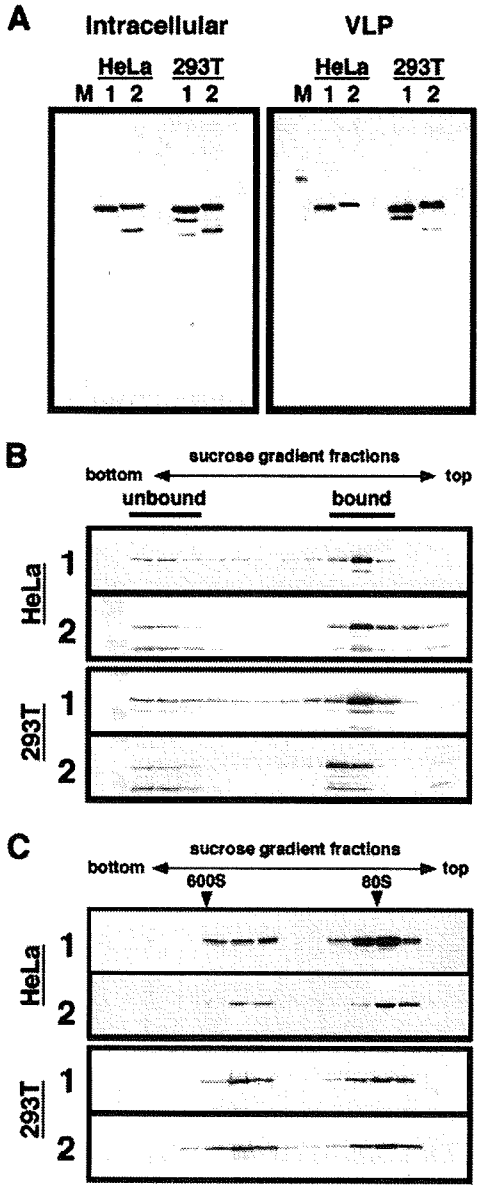

FIG. 6. Membrane association and multimerization of HIV-1 and HIV-2 Gags in higher eukaryotic cells. HeLa and 293T cells were transfected with a pCAGGS vector containing the HIV-1 or HIV-2 *gag* gene with a Flag epitope sequence, and after incubation at 37°C for 48 h, cells and culture medium were harvested for analysis. The culture medium was subjected to centrifugation on 20% sucrose cushions for purification of Gag VLPs. (A) Intracellular Gag expression and Gag VLP production. Transfected cells and Gag VLP fractions were subjected to SDS-PAGE followed by Western blotting using anti-Flag antibody. Lanes: M, molecular weight markers; 1 and 2, expression of HIV-1 and HIV-2 Gag-Flag, respectively. (B) Membrane affinity of Gag. Transfected cells were resuspended in buffer without NaCl and disrupted by sonication. Equilibrium flotation centrifugation and subsequent fractionation were carried out as described in the legend for Fig. 4. The gradient fractions were analyzed by Western blotting using anti-Flag antibody. Panels: 1, cells expressing HIV-1 Gag-Flag; 2, cells expressing HIV-2 Gag-Flag. (C) Sedimentation analysis of Gag. The whole-cell lysate was subjected to sedimentation analysis with a 20 to 70% sucrose gradient by centrifugation at 120,000 × *g* for 2 h, and gradient fractions were subjected to Western blotting using anti-Flag antibody. Panels: 1, cells expressing HIV-1 Gag-Flag; 2, cells expressing HIV-2 Gag-Flag. Arrowheads show sedimented positions of the immature form of HIV capsid (600S) and of 80S ribosomes.

membrane and formed high-order Gag multimers in higher eukaryotic cells and thus that no defect of particle production was observed.

The helix 2 region, but not the trimerization site, in HIV-2 MA abolishes high-order Gag assembly and subsequent particle production in yeast. To map a Gag region responsible for the failure of particle production in yeast, a series of chimeric Gag constructs between HIV-1 and HIV-2 were made (Fig. 7A) and expressed in yeast. Western blotting using anti-HIV-1 and anti-HIV-2 CA antibodies confirmed that each domain of Gag was replaced in the chimeric constructs. Spheroplast formation and VLP production were carried out as described above. Equivalent volumes of Gag VLP fractions were analyzed by SDS-PAGE followed by CBB staining. A failure of particle production was observed only when HIV-2 MA was present in the constructs (Fig. 7B, left panels). Further mapping experiments within MA indicated that the N-terminal one-third of HIV-2 MA (amino acid residues 1 to 44) is essentially responsible for the failure of VLP production (Fig. 7B, right panels). However, introduction of the corresponding region of HIV-1 MA into the HIV-2 background [construct M1(1/3)] did not rescue particle production, but a larger region of HIV-1 MA (the N-terminal half; residues 1 to 70) was required for particle production. Conversely, introduction of the N-terminal half of HIV-2 MA into the HIV-1 background [construct M2(1/2)] did not completely abolish particle production, but the introduction of a larger region of HIV-2 MA [construct M2(2/3)] did. These data suggest but do not prove that other sites affecting particle production may lie in the region between residues 45 and 96 and that the overall structural integrity of MA is not negligible.

Studies by nuclear magnetic resonance (25, 26) and crystallography (18, 38) have indicated that primate lentiviral MAs share three-dimensional characteristics, including the following: (i) the globular domain is composed of five helices (H1 to H5) capped by a β-sheet, in which the N-terminal basic residues are clustered; and (ii) in the MA trimer, the N-myristoyl moiety is inserted into a lipid bilayer and the surface-exposed basic residues come into contact with acidic phospholipids, such as phosphatidylinositol 4,5-bisphoshate [$PI(4,5)P_2$], in the membrane (18, 41). Indeed, the gross conformation of HIV-2 MA predicted by homology modeling using the SIVmac MA structure (38) as a template at Geno3D, an automated protein-modeling Web server (http://geno3d-pbil.ibcp.fr), is very similar to that of HIV-1 MA (see the supplemental material at http://www.kitasato-u.ac.jp/lisci/labo/ViralInfection2/1/Fig.S1.pdf), and the N-terminal half of MA (e.g., the cluster of basic amino acids) is relatively conserved between HIV-1 and HIV-2 compared with the C-terminal half (see the supplemental material at the website listed above), but our study found that the N-terminal half of MA is a determinant for Gag VLP production in yeast. To define the residues of MA critical for particle production in yeast, the clusters of nonconserved HIV-1 residues in the N-terminal half of MA were replaced with the corresponding HIV-2 residues (Fig. 8A), and the Gag constructs were expressed in yeast. Most of the substitutions had little effect on VLP production, and nearly equivalent levels of VLPs were produced even in the substitution mutant of the N-terminal trimerization site [construct 1(GLA)]. Interestingly, VLP production was severely impaired by the introduction of HIV-2 residues 38 to 40,

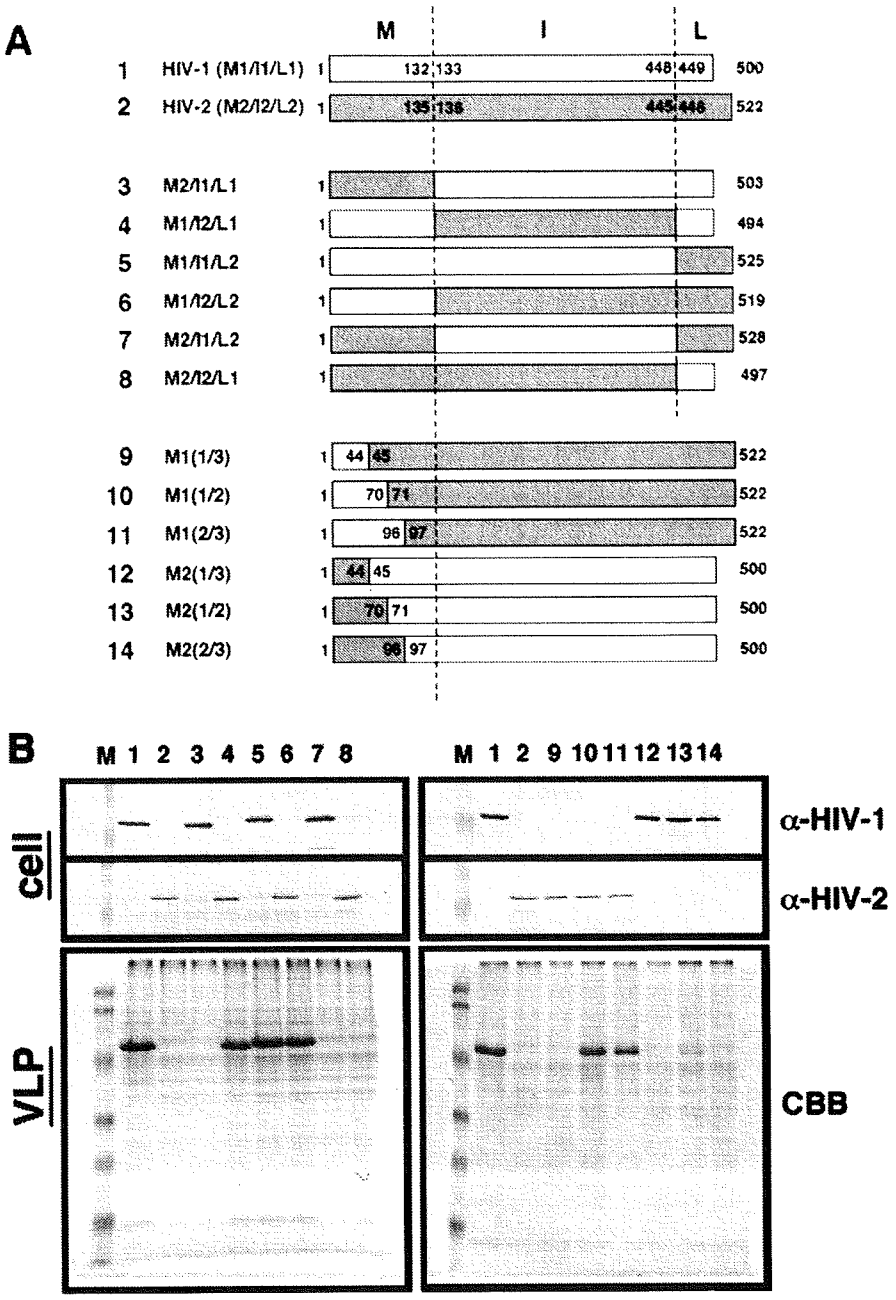

FIG. 7. Mapping of HIV-2 Gag regions inhibitory for Gag VLP production in yeast. (A) Schematic representation of chimeric Gags constructed between HIV-1 and HIV-2. (B) Intracellular Gag expression and Gag VLP production. Yeast cells were transformed with a pKT10 vector containing each Gag construct. Intracellular Gag expression was analyzed by Western blotting using anti-HIV-1 CA and anti-HIV-2 CA antibodies. Production and purification of Gag VLPs were carried out as described in the legend for Fig. 1. Gag VLPs were analyzed by SDS-PAGE followed by CBB staining. Lanes: M, prestained molecular weight markers; 1 and 2, expression of HIV-1 and HIV-2 Gag, respectively; 3 to 14, expression of chimeric Gags M2/I1/L1, M1/I2/L1, M1/I1/L2, M1/I2/L2, M2/I1/L2, M2/I2/L1, M1(1/3), M1(1/2), M1(2/3), M2(1/3), M2(1/2), and M2(2/3), respectively.

located near the end of helix 2 of MA, into HIV-1 Gag [construct 1(ANK)] (Fig. 8B). Introduction of the corresponding sequence of HIV-1 into HIV-2, however, did not confer particle production, although this was expected from the fact that the M1(1/3) construct did not produce Gag VLP (Fig. 7). We prepared the whole-cell lysates from several of the substitution mutants and examined their ability to form high-order Gag multimers by sedimentation analysis. The VLP-competent Gag mutants showed both high- and low-order Gag multimers, while in contrast, the VLP-incompetent Gag mutants showed only the low-order form (Fig. 8C). The 1(ANK) Gag construct did not show membrane affinity when samples were prepared in the absence of salt and subjected to membrane flotation analysis (Fig. 8D). These data indicate that a defined region of HIV-2 MA may affect stable

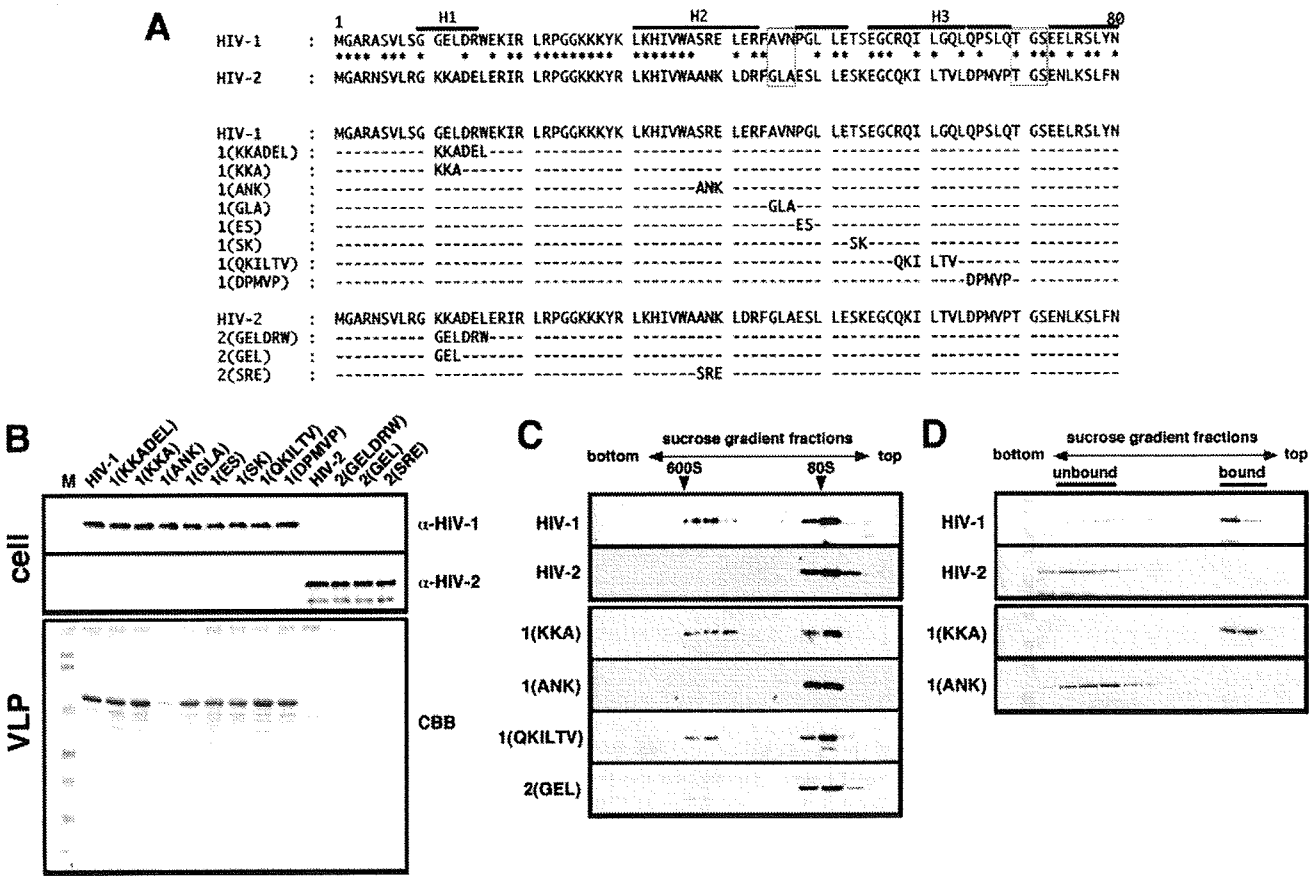

FIG. 8. Defining the N-terminal HIV-2 MA region inhibitory for Gag assembly and VLP production in yeast. (A) Amino acid alignment of Gag mutants with amino acid substitutions. The trimerization sites are shown in boxes, and helices 1 to 3 are shown as H1 to H3. (B) Intracellular expression and VLP production of Gag mutants. Protein expression and Gag VLP production in yeast were carried out as described in the legend for Fig. 1. Cell samples were subjected to Western blotting using anti-HIV-1 CA and anti-HIV-2 CA antibodies, and Gag VLPs were analyzed by SDS-PAGE followed by CBB staining. Lane M shows prestained molecular weight markers. (C) Sedimentation analysis of Gag mutants. Protein expression in yeast was carried out as described in the legend for Fig. 3. The whole-cell lysate was subjected to sedimentation analysis with a 20 to 70% sucrose gradient by centrifugation at 120,000 × *g* for 2 h, and gradient fractions were subjected to Western blotting using anti-Flag antibody. Arrowheads show sedimented positions of the immature form of HIV capsid (600S) and of 80S ribosomes. (D) Membrane affinities of Gag mutants in the absence of salt. Protein expression in yeast was carried out as described in the legend for Fig. 3, and equilibrium flotation centrifugation was described in the legend for Fig. 4. Gradient fractions were analyzed by Western blotting using anti-Flag antibody.

membrane affinity and high-order Gag assembly and, as a result, lead to the failure of VLP production in yeast.

DISCUSSION

The Gag proteins of primate lentiviral lineages have approximately 55 to 60% amino acid sequence identity between each of the lineages (8). In this study, we used Gag proteins of four different primate lentiviral lineages and analyzed their ability to produce Gag VLPs in yeast. We found that the Gag protein of the HIV-2/SIVmac lineage failed to release Gag VLPs in yeast, despite the fact that the Gag protein was myristoylated and targeted to the plasma membrane. The failure of HIV-2 Gag VLP production was likely due to the lack of high-order Gag multimerization but was also accompanied by an unstable association of Gag with the membrane. These findings were not observed in higher eukaryotic cells, suggesting that a host factor(s) was involved.

A host factor involved in Gag multimerization, ABCE1/HP68, has been identified by in vitro translation studies showing that this factor associates with relatively high-order Gag multimers but not with a lower-order form and facilitates Gag assembly into a VLP form as a molecular chaperone (56). Immunodepletion of ABCE1/HP68 in the in vitro reactions reduced the higher-order form with the accumulation of lower-order forms (56), a condition which was ostensibly similar to the failure of HIV-2 Gag assembly in yeast. However, this host factor is highly conserved in eukaryotes, including yeast, and has been shown to support all primate lentiviral Gag assembly (10). Later studies have shown that the NC but not MA domain is critical for Gag-ABCE1/HP68 interaction (23). From these data, it is unlikely that the putative host factor suggested in this study is ABCE1/HP68.

Primate lentiviral MA is composed of five helices, with helices 1 and 2 located on the upper surface of a globular MA structure in which the N-terminal basic residues are clustered.

In the MA trimer model, the myristoyl moiety and N-terminal basic residues act in synergy to stabilize the trimer on an acidic membrane (18). Recent studies have further indicated that $PI(4,5)P_2$, a lipid involved in membrane targeting of Gag (31), binds to a hydrophobic cleft formed with highly conserved amino acids by helices 2 and 4 and contributes to the membrane affinity of MA (41). Our data showed that the dominant region responsible for the failure of HIV-2 Gag VLP production was mapped near the end of helix 2 of MA, a site distinct from the MA trimerization site or the $PI(4,5)P_2$ binding cleft. The blockage of HIV-2 Gag VLP production in yeast occurred at the process of particle budding rather than Gag transport, and the membrane affinity of Gag was weakened. These facts suggest that such a host factor would be a component(s) including certain lipids present on or recruited to the plasma membrane, but the lipids would not be $PI(4,5)P_2$, and indeed, $PI(4,5)P_2$ is widely present in eukaryotes, including yeast. These data raise the alternative possibility that yeast may have an inhibitory factor(s) for HIV-2 Gag assembly.

Although it has been accepted that Gag oligomerization and membrane targeting are essentially independent events, recent studies have suggested that the membrane affinity of Gag may be promoted by Gag multimerization (43, 55). Another study indicated that the N-terminal myristoyl moiety of MA was exposed when MA formed a trimer (49). However, it is also possible that unstable membrane binding of Gag may not facilitate Gag multimerization, resulting in a lack of high-order assembly. In this study, we observed that the defects in Gag multimerization and membrane affinity occurred concomitantly in yeast, but we cannot prove, at present, which directly affected the failure of HIV-2 Gag VLP production in our system. In favor of the former possibility, the lack of a high-order Gag multimer was observed even at a physiological concentration of salt, a condition under which HIV-2 Gag associated with the yeast membrane. In contrast, the latter possibility would be supported by the data that (i) the region we mapped was located at helix 2 of MA, facing the membrane; (ii) in the MA trimer model (18, 38), this region is located near the center of the trimer, suggesting little possibility of involvement in higher-order Gag assembly; and (iii) the introduction of only three amino acids of HIV-2 Gag (located at the region) into the HIV-1 background, in which Gag multimerization domains are intact, failed to produce Gag VLPs.

The membrane affinity of Gag is regulated by N-myristoylation but also by the basic amino acid clusters in the M domain (4, 14, 15, 35, 54). In our study, the failure of HIV-2 Gag VLP production was accompanied by the dissociation of Gag from the membrane, a phenomenon which was observed only in the absence of salt. In general, relatively high concentrations of salt, such as 500 mM NaCl, disrupt electrostatic protein bonds but do not affect hydrophobic bonds. Conversely, in the absence of salt, hydrophobic but not electrostatic interactions are often disrupted. We observed that neither HIV-1 nor HIV-2 Gag dissociated from the membrane in the presence of 500 mM NaCl, suggesting that the N-terminal myristoyl moiety is a dominant determinant for membrane binding of Gag in yeast and that the membrane affinities of Gag mediated by the myristoyl moiety were comparable between the two Gags. In contrast, HIV-2 Gag dissociated from the yeast membrane in the absence of salt, under which condition HIV-1 Gag remained associated. These results suggest that the electrostatic interactions of HIV-2 Gag with the yeast membrane were weaker than those of HIV-1 Gag, leading to Gag dissociation from the yeast membrane. The amino acid sequences of the MA helix 2 region we mapped for the four primate lentiviral lineages are as follows: HIV-1, SRE; HIV-2, ANK; SIVmac, ANE; SIVagm, GKE; and SIVmnd, KGE.

Mutational studies of the N-terminal region of MA have suggested the involvement of hydrophobicity and electrostatic interactions of MA in Gag relocation and membrane extrusion. Amino acid substitutions in the MA basic domain redirected Gag to the endoplasmic reticulum and endosomes (34, 35, 54). Mutations of hydrophobic residues near the N terminus of MA to less hydrophobic residues severely impaired membrane binding of Gag without inhibiting N-terminal myristoylation, suggesting a failure of membrane insertion of the myristoyl moiety (36). Interestingly, in Mason-Pfizer monkey virus, a prototype for capsid formation prior to membrane relocation, an increase in the hydrophobicity of MA led to arrest at an early stage of particle budding, possibly by inhibiting exposure of the N-terminal myristoyl moiety (45). Thus, it cannot be ruled out that in our study, the absence of salt may have caused a disruption of the gross conformation of Gag (e.g., unfolding of the hydrophobic core of MA) and/or led to sequestration of the N-terminal myristoyl moiety.

ACKNOWLEDGMENTS

We thank S. Morikawa (National Institute of Infectious Diseases, Japan) for supply of the *gag* gene of SIVagm and the anti-SIVagm monkey serum and T. Miura (Kyoto University, Japan) for supply of the *gag* gene of SIVmnd. The cDNA of HIV-2 (ROD strain) was provided by the NIH AIDS Research and Reference Reagent Program. We also thank K. Mizumoto (Kitasato University, Japan) for supply of a yeast expression vector.

This work was supported by an AIDS grant from the Ministry of Health, Labor, and Welfare of Japan and by a grant-in-aid for scientific research from the Japan Society for the Promotion of Science.

REFERENCES

1. **Bagnat, M., S. Keranen, A. Shevchenko, and K. Simons.** 2000. Lipid rafts function in biosynthetic delivery of proteins to the cell surface in yeast. Proc. Natl. Acad. Sci. USA **97**:3254–3259.
2. **Bieniasz, P. D.** 2003. Restriction factors: a defense against retroviral infection. Trends Microbiol. **11**:286–291.
3. **Braaten, D., and J. Luban.** 2001. Cyclophilin A regulates HIV-1 infectivity, as demonstrated by gene targeting in human T cells. EMBO J. **20**:1300–1309.
4. **Bryant, M., and L. Ratner.** 1990. Myristoylation-dependent replication and assembly of human immunodeficiency virus 1. Proc. Natl. Acad. Sci. USA **87**:523–527.
5. **Campbell, S., and A. Rein.** 1999. In vitro assembly properties of human immunodeficiency virus type 1 Gag protein lacking the p6 domain. J. Virol. **73**:2270–2279.
6. **Campbell, S., and V. M. Vogt.** 1997. In vitro assembly of virus-like particles with Rous sarcoma virus Gag deletion mutants: identification of the p10 domain as a morphological determinant in the formation of spherical particles. J. Virol. **71**:4425–4435.
7. **Carriere, C., B. Gay, N. Chazal, N. Morin, and P. Boulanger.** 1995. Sequence requirements for encapsidation of deletion mutants and chimeras of human immunodeficiency virus type 1 Gag precursor into retrovirus-like particles. J. Virol. **69**:2366–2377.
8. **Desrosiers, R. C.** 1990. HIV-1 origins. A finger on the missing link. Nature **345**:288–289.
9. **Dong, X., H. Li, A. Derdowski, L. Ding, A. Burnett, X. Chen, T. R. Peters, T. S. Dermody, E. Woodruff, J. J. Wang, and P. Spearman.** 2005. AP-3 directs the intracellular trafficking of HIV-1 Gag and plays a key role in particle assembly. Cell **120**:663–674.
10. **Donher, J. E., and J. R. Lingappa.** 2004. Conservation of a stepwise, energy-sensitive pathway involving HP68 for assembly of primate lentivirus capsids in cells. J. Virol. **78**:1645–1656.
11. **Dorfman, T., A. Bukovsky, A. Ohagen, S. Hoglund, and H. G. Gottlinger.**

1994. Functional domains of the capsid protein of human immunodeficiency virus type 1. J. Virol. **68**:8180–8187.
12. **Garrus, J. E., U. K. von Schwedler, O. W. Pornillos, S. G. Morham, K. H. Zavitz, H. E. Wang, D. A. Wettstein, K. M. Stray, M. Cote, R. L. Rich, D. G. Myszka, and W. I. Sundquist.** 2001. Tsg101 and the vacuolar protein sorting pathway are essential for HIV-1 budding. Cell **107**:55–65.
13. **Gerrard, S. R., B. P. Levi, and T. H. Stevens.** 2000. Pep12p is a multifunctional yeast syntaxin that controls entry of biosynthetic, endocytic and retrograde traffic into the prevacuolar compartment. Traffic **1**:259–269.
14. **Gheysen, D., E. Jacobs, F. de Foresta, C. Thiriart, M. Francotte, D. Thines, and M. De Wilde.** 1989. Assembly and release of HIV-1 precursor $Pr55^{gag}$ virus-like particles from recombinant baculovirus-infected insect cells. Cell **59**:103–112.
15. **Gottlinger, H. G., J. G. Sodroski, and W. A. Haseltine.** 1989. Role of capsid precursor processing and myristoylation in morphogenesis and infectivity of human immunodeficiency virus type 1. Proc. Natl. Acad. Sci. USA **86**:5781–5785.
16. **Gottlinger, H. G., T. Dorfman, J. G. Sodroski, and W. A. Haseltine.** 1991. Effect of mutations affecting the p6 gag protein on human immunodeficiency virus particle release. Proc. Natl. Acad. Sci. USA **88**:3195–3199.
17. **Hahn, B. H., G. M. Shaw, K. M. De Cock, and P. M. Sharp.** 2000. AIDS as a zoonosis: scientific and public health implications. Science **287**:607–614.
18. **Hill, C. P., D. Worthylake, D. P. Bancroft, A. M. Christensen, and W. I. Sundquist.** 1996. Crystal structures of the trimeric human immunodeficiency virus type 1 matrix protein: implications for membrane association and assembly. Proc. Natl. Acad. Sci. USA **93**:3099–3104.
19. **Hoshikawa, N., A. Kojima, A. Yasuda, E. Takayashiki, S. Masuko, J. Chiba, T. Sata, and T. Kurata.** 1991. Role of the *gag* and *pol* genes of human immunodeficiency virus in the morphogenesis and maturation of retrovirus-like particles expressed by recombinant vaccinia virus: an ultrastructural study. J. Gen. Virol. **72**:2509–2517.
20. **Keckesova, Z., L. M. Ylinen, and G. J. Towers.** 2004. The human and African green monkey TRIM5alpha genes encode Ref1 and Lv1 retroviral restriction factor activities. Proc. Natl. Acad. Sci. USA **101**:10780–10785.
21. **Kikonyogo, A., F. Bouamr, M. L. Vana, Y. Xiang, A. Aiyar, C. Carter, and J. Leis.** 2001. Proteins related to the Nedd4 family of ubiquitin protein ligases interact with the L domain of Rous sarcoma virus and are required for gag budding from cells. Proc. Natl. Acad. Sci. USA **98**:11199–11204.
22. **Klikova, M., S. S. Rhee, E. Hunter, and T. Ruml.** 1995. Efficient in vivo and in vitro assembly of retroviral capsids from Gag precursor proteins expressed in bacteria. J. Virol. **69**:1093–1098.
23. **Lingappa, J. R., J. E. Dooher, M. A. Newman, P. K. Kiser, and K. C. Klein.** 2006. Basic residues in the nucleocapsid domain of Gag are required for interaction of HIV-1 Gag with ABCE1 (HP68), a cellular protein important for HIV-1 capsid assembly. J. Biol. Chem. **281**:3773–3784.
24. **Mammano, F., A. Ohagen, S. Hoglund, and H. G. Gottlinger.** 1994. Role of the major homology region of human immunodeficiency virus type 1 in virion morphogenesis. J. Virol. **68**:4927–4936.
25. **Massiah, M. A., M. R. Starich, C. Paschall, M. F. Summers, A. M. Christensen, and W. I. Sundquist.** 1994. Three-dimensional structure of the human immunodeficiency virus type 1 matrix protein. J. Mol. Biol. **244**:198–223.
26. **Matthews, S., P. Barlow, J. Boyd, G. Barton, R. Russell, H. Mills, M. Cunningham, N. Meyers, N. Burns, N. Clark, S. Kingsman, A. Kingsman, and I. Campbell.** 1994. Structural similarity between the p17 matrix protein of HIV-1 and interferon-gamma. Nature **370**:666–668.
27. **Morikawa, Y., T. Goto, and K. Sano.** 1999. *In vitro* assembly of human immunodeficiency virus type 1 Gag protein. J. Biol. Chem. **274**:27997–28002.
28. **Morikawa, Y., T. Goto, and F. Momose.** 2004. Human immunodeficiency virus type 1 Gag assembly through assembly intermediates. J. Biol. Chem. **279**:31964–31972.
29. **Nguyen, D. H., and J. E. Hildreth.** 2000. Evidence for budding of human immunodeficiency virus type 1 selectively from glycolipid-enriched membrane lipid rafts. J. Virol. **74**:3264–3272.
30. **Niwa, H., K. Yamamura, and J. Miyazaki.** 1991. Efficient selection for high-expression transfectants with a novel eukaryotic vector. Gene **108**:193–199.
31. **Ono, A., S. D. Ablan, S. J. Lockett, K. Nagashima, and E. O. Freed.** 2004. Phosphatidylinositol (4,5) bisphosphate regulates HIV-1 Gag targeting to the plasma membrane. Proc. Natl. Acad. Sci. USA **101**:14889–14894.
32. **Ono, A., and E. O. Freed.** 1999. Binding of human immunodeficiency virus type 1 Gag to membrane: role of the matrix amino terminus. J. Virol. **73**:4136–4144.
33. **Ono, A., and E. O. Freed.** 2001. Plasma membrane rafts play a critical role in HIV-1 assembly and release. Proc. Natl. Acad. Sci. USA **98**:13925–13930.
34. **Ono, A., and E. O. Freed.** 2004. Cell-type-dependent targeting of human immunodeficiency virus type 1 assembly to the plasma membrane and the multivesicular body. J. Virol. **78**:1552–1563.
35. **Ono, A., J. M. Orenstein, and E. O. Freed.** 2000. Role of the Gag matrix domain in targeting human immunodeficiency virus type 1 assembly. J. Virol. **74**:2855–2866.
36. **Paillart, J. C., and H. G. Gottlinger.** 1999. Opposing effects of human immunodeficiency virus type 1 matrix mutations support a myristyl switch model of Gag membrane targeting. J. Virol. **73**:2604–2612.
37. **Parent, L. J., R. P. Bennett, R. C. Craven, T. D. Nelle, N. K. Krishna, J. B. Bowzard, C. B. Wilson, B. A. Puffer, R. C. Montelaro, and J. W. Wills.** 1995. Positionally independent and exchangeable late budding functions of the Rous sarcoma virus and human immunodeficiency virus Gag proteins. J. Virol. **69**:5455–5460.
38. **Rao, Z., A. S. Belyaev, E. Fry, P. Roy, I. M. Jones, and D. I. Stuart.** 1995. Crystal structure of SIV matrix antigen and implications for virus assembly. Nature **378**:743–747.
39. **Reicin, A. S., S. Paik, R. D. Berkowitz, J. Luban, I. Lowy, and S. P. Goff.** 1995. Linker insertion mutations in the human immunodeficiency virus type 1 *gag* gene: effects on virion particle assembly, release, and infectivity. J. Virol. **69**:642–650.
40. **Ruggieri, R., K. Tanaka, M. Nakafuku, Y. Kaziro, A. Toh-e, and K. Matsumoto.** 1989. *MSI1*, a negative regulator of the RAS-cAMP pathway in *Saccharomyces cerevisiae*. Proc. Natl. Acad. Sci. USA **86**:8778–8782.
41. **Saad, J. S., J. Miller, J. Tai, A. Kim, R. H. Ghanam, and M. F. Summers.** 2006. Structural basis for targeting HIV-1 Gag proteins to the plasma membrane for virus assembly. Proc. Natl. Acad. Sci. USA **103**:11364–11369.
42. **Sakuragi, S., T. Goto, K. Sano, and Y. Morikawa.** 2002. HIV type 1 Gag virus-like particle budding from spheroplasts of *Saccharomyces cerevisiae*. Proc. Natl. Acad. Sci. USA **99**:7956–7961.
43. **Sandefur, S., V. Varthakavi, and P. Spearman.** 1998. The I domain is required for efficient plasma membrane binding of human immunodeficiency virus type 1 Pr55Gag. J. Virol. **72**:2723–2732.
44. **Smith, A. J., N. Srinivasakumar, M. L. Hammarskjold, and D. Rekosh.** 1993. Requirements for incorporation of $Pr160^{gag\text{-}pol}$ from human immunodeficiency virus type 1 into virus-like particles. J. Virol. **67**:2266–2275.
45. **Stansell, E., E. Tytler, M. R. Walter, and E. Hunter.** 2004. An early stage of Mason-Pfizer monkey virus budding is regulated by the hydrophobicity of the Gag matrix domain core. J. Virol. **78**:5023–5031.
46. **Strack, B., A. Calistri, S. Craig, E. Popova, and H. G. Gottlinger.** 2003. AIP1/ALIX is a binding partner for HIV-1 p6 and EIAV p9 functioning in virus budding. Cell **114**:689–699.
47. **Stremlau, M., C. M. Owens, M. J. Perron, M. Kiessling, P. Autissier, and J. Sodroski.** 2004. The cytoplasmic body component TRIM5alpha restricts HIV-1 infection in Old World monkeys. Nature **427**:848–853.
48. **Tanaka, K., M. Nakafuku, F. Tamanoi, Y. Kaziro, K. Matsumoto, and A. Toh-e.** 1990. *IRA2*, a second gene of *Saccharomyces cerevisiae* that encodes a protein with a domain homologous to mammalian *ras* GTPase-activating protein. Mol. Cell. Biol. **10**:4303–4313.
49. **Tang, C., E. Loeliger, P. Luncsford, I. Kinde, D. Beckett, and M. F. Summers.** 2004. Entropic switch regulates myristate exposure in the HIV-1 matrix protein. Proc. Natl. Acad. Sci. USA **101**:517–522.
50. **Towers, G. J., T. Hatziioannou, S. Cowan, S. P. Goff, J. Luban, and P. D. Bieniasz.** 2003. Cyclophilin A modulates the sensitivity of HIV-1 to host restriction factors. Nat. Med. **9**:1138–1143.
51. **Towler, D. A., S. P. Adams, S. R. Eubanks, D. S. Towery, E. Jackson-Machelski, L. Glaser, and J. I. Gordon.** 1988. Myristoyl CoA: protein N-myristoyltransferase activities from rat liver and yeast possess overlapping yet distinct peptide substrate specificities. J. Biol. Chem. **263**:1784–1790.
52. **VerPlank, L., F. Bouamr, T. J. LaGrassa, B. Agresta, A. Kikonyogo, J. Leis, and C. A. Carter.** 2001. Tsg101, a homologue of ubiquitin-conjugating (E2) enzymes, binds the L domain in HIV type 1 Pr55(Gag). Proc. Natl. Acad. Sci. USA **98**:7724–7729.
53. **von Schwedler, U. K., M. Stuchell, B. Muller, D. M. Ward, H. Y. Chung, E. Morita, H. E. Wang, T. Davis, G. P. He, D. M. Cimbora, A. Scott, H. G. Krausslich, J. Kaplan, S. G. Morham, and W. I. Sundquist.** 2003. The protein network of HIV budding. Cell **114**:701–713.
54. **Yuan, X., X. Yu, T. H. Lee, and M. Essex.** 1993. Mutations in the N-terminal region of human immunodeficiency virus type 1 matrix protein block intracellular transport of the Gag precursor. J. Virol. **67**:6387–6394.
55. **Zhou, W., and M. D. Resh.** 1996. Differential membrane binding of the human immunodeficiency virus type 1 matrix protein. J. Virol. **70**:8540–8548.
56. **Zimmerman, C., K. C. Klein, P. K. Kiser, A. R. Singh, B. L. Firestein, S. C. Riba, and J. R. Lingappa.** 2002. Identification of a host protein essential for assembly of immature HIV-1 capsids. Nature **415**:88–92.

JOURNAL OF VIROLOGY, Nov. 2007, p. 11640–11649 Vol. 81, No. 21
0022-538X/07/$08.00+0 doi:10.1128/JVI.01475-07

Induction of CD8$^+$ Cells Able To Suppress CCR5-Tropic Simian Immunodeficiency Virus SIVmac239 Replication by Controlled Infection of CXCR4-Tropic Simian-Human Immunodeficiency Virus in Vaccinated Rhesus Macaques$^\nabla$

Tetsuo Tsukamoto,[1,2]† Mitsuhiro Yuasa,[1]† Hiroyuki Yamamoto,[1] Miki Kawada,[1,2] Akiko Takeda,[1] Hiroko Igarashi,[2] and Tetsuro Matano[1,2,3,4]*

International Research Center for Infectious Diseases, The Institute of Medical Science, The University of Tokyo, 4-6-1 Shirokanedai, Minato-Ku, Tokyo 108-8639, Japan[1]; Graduate School of Medicine, The University of Tokyo, 7-3-1 Hongo, Bunkyo-Ku, Tokyo 113-0033, Japan[2]; AIDS Research Center, National Institute of Infectious Diseases, 1-23-1 Toyama, Shinjuku-ku, Tokyo 162-8640, Japan[3]; and Tsukuba Primate Research Center, National Institute of Biomedical Innovation, 1 Hachimandai, Tsukuba, Ibaraki 305-0843, Japan[4]

Received 5 July 2007/Accepted 16 August 2007

Recent recombinant viral vector-based AIDS vaccine trials inducing cellular immune responses have shown control of CXCR4-tropic simian-human immunodeficiency virus (SHIV) replication but difficulty in containment of pathogenic CCR5-tropic simian immunodeficiency virus (SIV) in rhesus macaques. In contrast, controlled infection of live attenuated SIV/SHIV can confer the ability to contain SIV superchallenge in macaques. The specific immune responses responsible for this control may be induced by live virus infection but not consistently by viral vector vaccination, although those responses have not been determined. Here, we have examined in vitro anti-SIV efficacy of CD8$^+$ cells in rhesus macaques that showed prophylactic viral vector vaccine-based control of CXCR4-tropic SHIV89.6PD replication. Analysis of the effect of CD8$^+$ cells obtained at several time points from these macaques on CCR5-tropic SIVmac239 replication in vitro revealed that CD8$^+$ cells in the chronic phase after SHIV challenge suppressed SIV replication more efficiently than those before challenge. SIVmac239 superchallenge of two of these macaques at 3 or 4 years post-SHIV challenge was contained, and the following anti-CD8 antibody administration resulted in transient CD8$^+$ T-cell depletion and appearance of plasma SIVmac239 viremia in both of them. Our results indicate that CD8$^+$ cells acquired the ability to efficiently suppress SIV replication by controlled SHIV infection, suggesting the contribution of CD8$^+$ cell responses induced by controlled live virus infection to containment of HIV/SIV superinfection.

Live attenuated immunodeficiency virus infection can induce effective immune responses against pathogenic human immunodeficiency virus type 1 (HIV-1) and simian immunodeficiency virus (SIV) replication, although concerns about conditions necessary for its safety as an AIDS vaccine have not been satisfied at present (3, 13, 19). In macaque AIDS models, infection of live attenuated viruses such as SIVmac239Δnef, SIVmac239Δ3, and simian-human immunodeficiency virus (SHIV) 89.6 have been shown to confer potent immune responses resulting in control of SIV superchallenge (7, 14, 35, 53). While involvement of virus-specific CD8$^+$ cytotoxic T-lymphocyte (CTL) responses has been indicated, it has remained unclear what immune responses play a key role in this control (19, 34).

Virus-specific cellular immune responses are crucial for control of HIV-1 and SIV infections (1, 4, 5, 10, 12, 20, 29, 38, 41, 42). Recombinant viral vector-based vaccines efficiently eliciting virus-specific cellular immune responses have been developed as promising AIDS vaccine candidates (32). These prophylactic vaccine trials in rhesus macaques have shown viral control and prevention of acute CD4$^+$ T-cell depletion after CXCR4-tropic SHIV challenge (2, 27, 36, 37, 40, 46). Unfortunately, however, trials of these vaccines have shown difficulty in containment of CCR5-tropic SIV infection that induces acute, massive depletion of CCR5$^+$ CD4$^+$ memory T cells and chronic disease progression like HIV-1 infection in humans (6, 8, 11, 21, 23, 28, 30, 31, 39, 49, 50, 52). Possibly, the specific immune responses responsible for SIV control might be induced by live SIV/SHIV infection but not consistently by recombinant viral vector vaccination. Previous CD8$^+$ cell-depletion experiments in macaques using a monoclonal anti-CD8 antibody have indicated the importance of CD8$^+$ cells in SIV control (12, 29, 42), but differences in antiviral efficacy between live SIV/SHIV infection-induced and recombinant viral vector vaccination-induced CD8$^+$ cells have not been determined.

Our previous trials of a prophylactic vaccine using a Gag-expressing Sendai virus (SeV-Gag) vector have shown control of CXCR4-tropic SHIV89.6PD replication in vaccinated rhesus macaques (27, 47). While this vaccination did not always result in CCR5-tropic SIVmac239 control (28), it was speculated that, after SHIV challenge, these vaccinees may possibly

* Corresponding author. Mailing address: International Research Center for Infectious Diseases, The Institute of Medical Science, The University of Tokyo, 4-6-1 Shirokanedai, Minato-ku, Tokyo 108-8639, Japan. Phone: 81-3-6409-2078. Fax: 81-3-6409-2076. E-mail: matano@m.u-tokyo.ac.jp.

† T.T. and M.Y. contributed equally to this work.

$^\nabla$ Published ahead of print on 29 August 2007.

TABLE 1. Virus challenge and antibody administration schedule

Macaque	Prophylactic vaccination	Time (wk) of:			
		SHIV89.6PD challenge	Anti-CD20 monoclonal antibody administration	SIVmac239 superchallenge	Anti-CD8 monoclonal antibody administration
R00-017	SeV-Gag	0	166	203	209
R00-020	DNA prime with SeV-Gag boost	0	140	151	163
R00-023	DNA prime with SeV-Gag boost	0			
R00-024	DNA prime with SeV-Gag boost	0			

acquire the potential for controlling SIVmac239 superchallenge. In the present study, we have examined whether these SHIV controllers acquired $CD8^+$ cells effective against SIVmac239 replication. Our analyses have suggested that $CD8^+$ cell responses capable of suppressing SIVmac239 replication in vitro were induced by controlled SHIV infection and that these responses might be crucial for control of superchallenged SIVmac239 replication.

MATERIALS AND METHODS

Animal experiments. Four Burmese rhesus macaques (*Macaca mulatta*) used in this study (Table 1) were maintained in accordance with the *Guides for Animal Experiments Performed at National Institute of Infectious Diseases* (35a). Blood collection, vaccination, virus challenge, and antibody administration were performed under ketamine anesthesia. These macaques received prophylactic vaccination and SHIV89.6PD challenge as described in our previous studies (27, 47). Macaque R00-017 was vaccinated intranasally with 1×10^8 cell infectious units (CIU) of replication-competent SeV-Gag vector (15, 16), whereas macaques R00-020, R00-023, and R00-024 were primed intramuscularly with 5 mg of cytomegalovirus (CMV)-SHIVdEN DNA and then boosted intranasally with 6×10^9 CIU of replication-defective F-deleted SeV-Gag vector (22). The CMV-SHIVdEN DNA was constructed from an *env*- and *nef*-deleted $SHIV_{MD14YE}$ molecular clone DNA (45) and has the genes encoding SIVmac239 Gag, Pol, Vif, and Vpx; SIVmac239-HIV-1_{DH12} chimeric Vpr; and HIV-1_{DH12} Tat and Rev as described previously (28, 47). These vaccinees were challenged intravenously with 10 50% tissue culture infective doses ($TCID_{50}$) of SHIV89.6PD (25) 13 weeks (in R00-020, R00-023, and R00-024) or 14 weeks (in R00-017) after SeV-Gag vaccination.

Macaques R00-023 and R00-024 were euthanized around 2 years after SHIV89.6PD challenge, while macaques R00-017 and R00-020 were followed up for more than 2 years. The latter two animals received monoclonal anti-CD20 antibody administration for $CD20^+$ cell depletion (starting at week 166 in R00-017 and week 140 in R00-020), intravenous superchallenge with 1,000 $TCID_{50}$ of SIVmac239 (18) (at week 203 in R00-017 and week 151 in R00-020), and monoclonal anti-CD8 antibody administration for $CD8^+$ cell depletion (starting at week 209 in R00-017 and week 163 in R00-020) (Table 1). For $CD20^+$ cell depletion, animals were inoculated intravenously with 10 mg/kg of monoclonal anti-CD20 antibody (Rituximab; Zenyaku Kogyo, Tokyo, Japan) four times every other week. Peripheral B-cell depletion was confirmed by immunostaining using anti-human CD19 antibody and anti-human CD20 antibody (Becton Dickinson, Tokyo, Japan). For $CD8^+$ cell depletion, animals received a single subcutaneous inoculation of 10 mg/kg of monoclonal anti-CD8 antibody (cM-T807) provided by Centocor (Malvern, PA) followed by three intravenous inoculations of 5 mg/kg cM-T807 on days 3, 7, and 10 after the first inoculation. Peripheral $CD8^+$ T-cell depletion was confirmed by immunostaining using anti-human CD8 antibody (DK25; Dako, Kyoto, Japan). Macaques R00-017 and R00-020 were euthanized 3 months after the anti-CD8 antibody administration.

Quantitation of plasma viral loads. Plasma RNA was extracted using the High Pure viral RNA kit (Roche Diagnostics, Tokyo, Japan). For quantitation of plasma SIV/SHIV RNA levels, serial fivefold dilutions of RNA samples were amplified in quadruplicate by reverse transcription (RT) and nested PCR to determine the endpoint. SIV *gag*-specific primers (AGAAACTCCGTCTTGT CAGG and TGATAATCTGCATAGCCGC for the first RT-PCR and GATTA GCAGAAAGCCTGTTGG and TGCAACCTTCTGACAGTGC for the second DNA PCR) (Sigma-Aldrich, Tokyo, Japan) that recognize the *gag* region shared by SHIV89.6PD and SIVmac239 were used. Plasma SIV/SHIV RNA levels were calculated according to the Reed-Muench method as described previously (28). The lower limit of detection in this assay is approximately 4×10^2 copies/ml. After SIVmac239 superchallenge, plasma SIVmac239 RNA levels were measured by the LightCycler system (Roche Diagnostics) using SIVmac239 *env*-specific primers (AAGAATTGTTGCGACTGACC and CAGTAGTGTGGCA GACTTGTC) and probes (CATTCAGCTGCGCCTGGTCCTTTAAGTAC-Flu and LcRed-TCTTCGATGGCAGTGACCCTAGTCTGGAGG) (Nihon Gene Research Laboratories, Inc., Sendai, Japan) that recognize SIVmac239 *env* but not SHIV89.6PD *env*. SHIV89.6PD RNA levels were also measured using SHIV89.6PD *env*-specific primers (GGATGTTGATGATCTGTAGTGC and CCAATACTACTTCTTGTGGGTT) and probes (CAGTCTATTATGGGG TACCTGTGTGGAGAGAAGCA-Flu and LcRed-CCACCACTCTATTTT GTGCATCAGATGCTAAAGCC) that recognize SHIV89.6PD *env* but not SIVmac239 *env*. The lower limit of detection in this assay is approximately 1×10^3 copies/ml.

In vitro viral suppression assay. We examined SIVmac239 replication on CD8-depleted peripheral blood mononuclear cells (PBMCs) in the presence of $CD8^+$ cells positively selected from PBMCs. Macaque PBMCs prepared from blood at several time points were frozen and stored until use. Thawed PBMCs were separated into $CD8^+$ cells and $CD8^-$ cells by using MACS CD8 MicroBeads (Miltenyi Biotec, Tokyo, Japan). The purity of the former was more than 96%, while the latter included less than 3% of $CD8^+$ cells. To prepare target cells, one fifth of $CD8^-$ cells negatively selected from PBMCs obtained before SHIV89.6PD challenge were infected with SIVmac239 at a multiplicity of infection (MOI) of $1:10^4$, and these infected cells and the remaining uninfected $CD8^-$ cells were cultured separately in the presence of 2 μg/ml phytohemagglutinin-L (Roche Diagnostics). After a 48-h culture, both infected and uninfected $CD8^-$ cells were collected, washed three times, and mixed to be used as target cells. Then, 4×10^5 target cells were cultured alone or cocultured with 4×10^5 (effector/target [E:T] ratio of 1:1) or 4×10^4 (E:T ratio of 1:10) $CD8^-$ effector cells positively selected from PBMCs in a well of 96-well flat-bottom plate and the culture supernatants were harvested every other day for measurement of SIV Gag CA p27 concentration by SIV core antigen enzyme-linked immunosorbent assay (ELISA) (Beckman Coulter, Tokyo, Japan). RPMI 1640 medium (Invitrogen, Tokyo, Japan) supplemented with 10% heat-inactivated fetal bovine serum (HyClone, Logan, UT) and 20 IU/ml recombinant human interleukin-2 (Roche Diagnostics) were used for cell culture. All of the cocultures were in duplicate, and the mean value of p27 concentrations at each time point is shown.

Measurement of virus-specific $CD8^+$ T-cell responses. We measured virus-specific T-cell levels by flow cytometric analysis of gamma interferon (IFN-γ) induction after specific stimulation as described previously (27, 28). PBMCs were cocultured with autologous herpesvirus papio-immortalized B-lymphoblastoid cell lines (B-LCL) (51) infected with vesicular stomatitis virus G (VSV-G)-pseudotyped SIVGP1 for SIVGP1-specific stimulation. The VSV-G-pseudotyped SIVGP1 was obtained by cotransfection of COS-1 cells with pVSV-G (Clontech, Otsu, Japan) and SIVGP1, an *env*- and *nef*-deleted $SHIV_{MD14}$ molecular clone DNA (28, 45). Intracellular IFN-γ staining was performed using a Cytofix-Cytoperm kit (Becton Dickinson). Peridinin chlorophyll-conjugated anti-human CD8, allophycocyanin-conjugated anti-human CD3, and phycoerythrin-conjugated anti-human IFN-γ antibodies (Becton Dickinson) were used. Specific T-cell levels were calculated by subtracting the IFN-γ T-cell frequencies after nonspecific stimulation from those after SIVGP1-specific stimulation.

Measurement of virus-specific neutralizing titers. We measured virus-specific neutralizing titers as described previously (17, 44). Serial twofold dilutions of heat-inactivated plasma were prepared in duplicate and mixed with 10 $TCID_{50}$ of SIVmac239 or SHIV89.6PD. In each mixture, 5 μl of diluted plasma was incubated with 5 μl of virus. After a 45-min incubation at room temperature, each 10-μl mixture was added to 5×10^4 MT-4 cells in a well of a 96-well flat-bottom

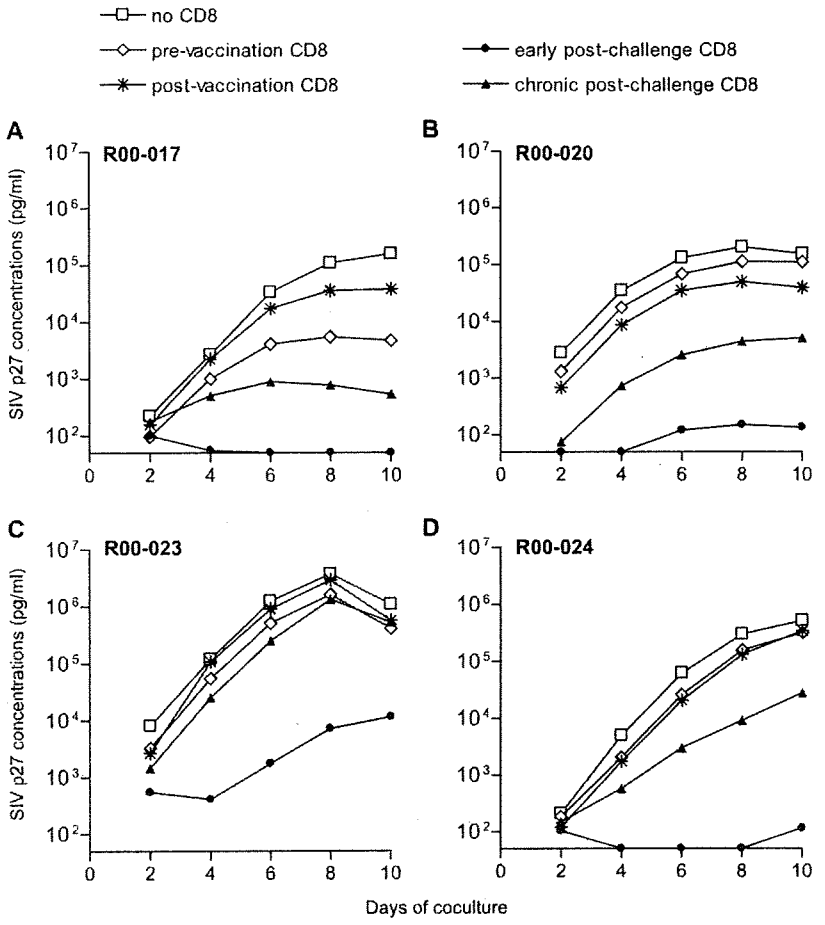

	R00-017	R00-020	R00-023	R00-024
post-vaccination	wks -6 & -4	wks -11 & -4	wk -7	wks -11 & -6
early post-challenge	wks 3 & 5	wks 5 & 8	wk 5	wks 5 & 13
chronic post-challenge	wk 67	wks 52 & 63	wk 30	wks 52 & 63

FIG. 1. SIVmac239 replication in vitro in the absence or the presence of $CD8^+$ cells in macaques R00-017 (A), R00-020 (B), R00-023 (C), and R00-024 (D). PBMC-derived $CD8^-$ (target) cells infected with SIVmac239 were cultured alone (no CD8) or cocultured with autologous PBMC-derived $CD8^-$ (effector) cells obtained prevaccination (pre-vaccination CD8), postvaccination and pre-SHIV challenge (post-vaccination CD8), in the early phase post-SHIV challenge (early post-challenge CD8), or in the chronic phase post-SHIV challenge (chronic post-challenge CD8) at an E:T ratio of 1:1. A representative result of two sets of experiments with similar patterns is shown in panels A and D, whereas the result of a single experiment is shown in panels B and C. Postvaccination and postchallenge $CD8^+$ cells were prepared from PBMCs obtained at different time points, as shown in the bottom table (weeks before [shown by minus] or after SHIV challenge), because of a limitation of available samples. SeV-Gag vaccination was performed 13 weeks (in R00-020, R00-023, and R00-024) or 14 weeks (in R00-017) before SHIV challenge. In some groups, CD8 cells at two time points were mixed to prepare enough cells. p27 concentrations in the culture supernatants were examined by ELISA.

plate. After 12 days of culture, supernatants were harvested. Progeny virus production in the supernatants was examined by SIV core antigen ELISA for detection of SIV p27 to determine the 100% neutralizing end point. The lower limit of detection is a titer of 1:2.

RESULTS

Potency of $CD8^+$ cells post-SHIV challenge for suppressing SIVmac239 replication in vitro. We established a method for examining SIVmac239 replication in vitro in the presence of $CD8^+$ cells and evaluated the effect of $CD8^+$ cells on SIVmac239 replication in vitro in four rhesus macaques that showed vaccine-based containment of SHIV89.6PD challenge (Table 1). One of them (R00-017) received a single intranasal SeV-Gag vaccination, while the other three (R00-020, R00-023, and R00-024) received a single intramuscular DNA priming followed by a single intranasal SeV-Gag booster before SHIV89.6PD challenge as described previously (27, 47). All four of these macaques controlled viral replication with undetectable plasma viremia after the acute phase for more than 2 years post-SHIV89.6PD challenge (54).

From each animal, we prepared four groups of bulk $CD8^+$ cells obtained prevaccination, post-SeV-Gag vaccination (pre-SHIV challenge), in the early phase post-SHIV challenge (weeks 3 to 8), and in the chronic phase post-SHIV challenge

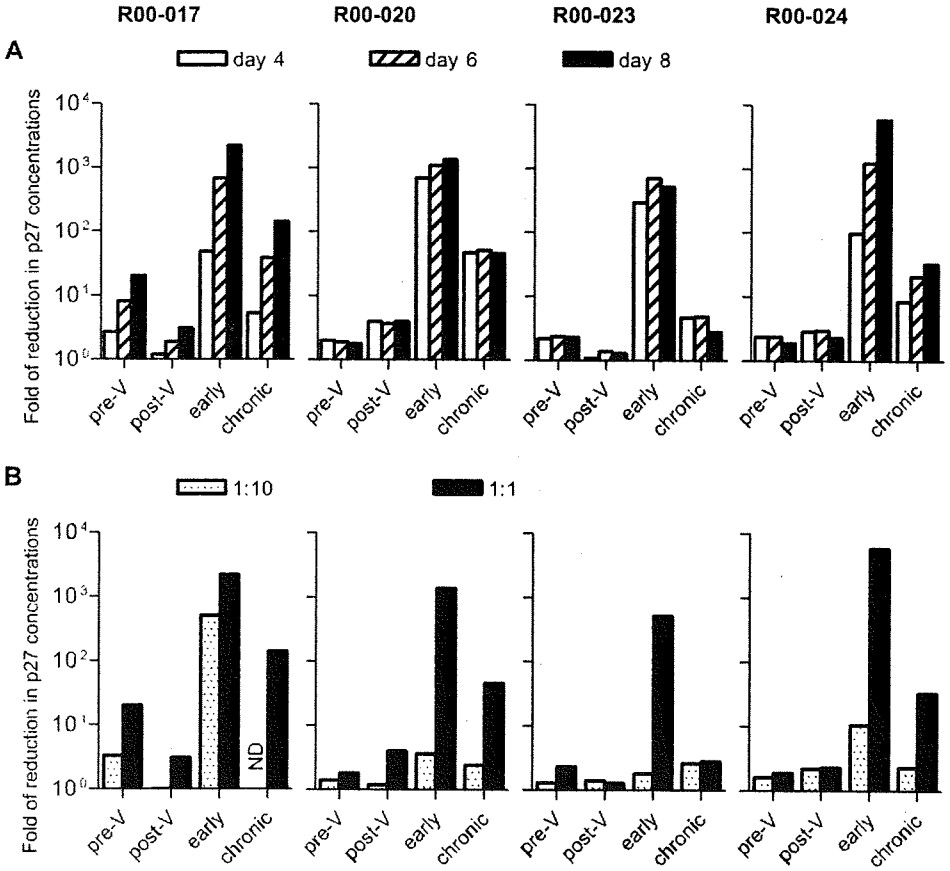

FIG. 2. Reduction in SIVmac239 production by addition of $CD8^+$ cells. The reduction (fold) in p27 concentration in the supernatant from coculture of SIV-infected $CD8^-$ cells with each group of $CD8^+$ cells compared to that from SIV-infected $CD8^-$ cell culture without $CD8^+$ cells is shown. (A) Reduction in p27 concentration on days 4, 6, and 8 of coculture at an E:T ratio of 1:1 (calculated from the data in Fig. 1). (B) Reduction in p27 concentration on day 8 of coculture at an E:T ratio of 1:1 (black bars) or 1:10 (dotted bars). pre-V, prevaccination CD8; post-V, postvaccination CD8; early, early postchallenge CD8; chronic, chronic postchallenge CD8 as described in the legend to Fig. 1. ND, not determined.

(weeks 30 to 67). These groups of effector $CD8^+$ cells were cocultured with SIVmac239-infected autologous target $CD8^-$ cells at the E:T ratio of 1:1, and p27 concentrations in the culture supernatants were measured for evaluation of SIVmac239 production (Fig. 1). Reduction in SIVmac239 production by addition of each group of $CD8^+$ cells was shown as reduction (fold) in p27 concentration compared to that in the supernatant from the SIVmac239-infected $CD8^-$ cell culture without $CD8^+$ cells (Fig. 2A).

Even addition of prevaccination $CD8^+$ cells resulted in reduction of SIV production. Especially, prevaccination $CD8^+$ cells derived from macaque R00-017 efficiently suppressed SIV replication, showing an approximately 20-fold reduction in viral production at day 8 of culture. In other three macaques, however, the reduction in SIV production by addition of prevaccination $CD8^+$ cells was less than threefold. In macaque R00-020, postvaccination/prechallenge $CD8^+$ cells suppressed SIV replication more efficiently than prevaccination ones, but in the other three macaques, the levels of suppression by postvaccination/prechallenge $CD8^+$ cells were not more than those by prevaccination cells.

In contrast, $CD8^+$ cells in the early phase postchallenge showed an efficient suppressive effect on SIV replication in all four macaques. Maximum reduction (fold) in SIV production by addition of these $CD8^+$ cells was more than 7×10^2. Addition of $CD8^+$ cells in the chronic phase postchallenge also resulted in efficient reduction of SIV production. The levels of reduction were lower than those by $CD8^+$ cells in the early phase postchallenge but higher than those by prechallenge $CD8^+$ cells. Thus, all four vaccinees, after SHIV challenge, acquired $CD8^+$ cells able to suppress SIVmac239 replication in vitro efficiently. Efficient reduction by early postchallenge $CD8^+$ cells was observed in some animals even at the E:T ratio of 1:10 (Fig. 2B).

We then measured SIVGP1-specific $CD8^+$ T-cell frequencies in PBMCs by detection of IFN-γ induction after stimulation with B-LCL expressing an *env*- and *nef*-deleted SHIV molecular clone (SIVGP1) DNA (27, 28) (Fig. 3). In all four macaques, SIVGP1-specific $CD8^+$ T-cell levels peaked during the acute phase post-SHIV challenge and gradually decreased after the set point. SIVGP1-specific $CD8^-$ T-cell frequencies after the acute phase were higher in macaques R00-017 and R00-023 compared to those post-SeV-Gag vaccination (prechallenge) but interestingly lower in macaque R00-020.

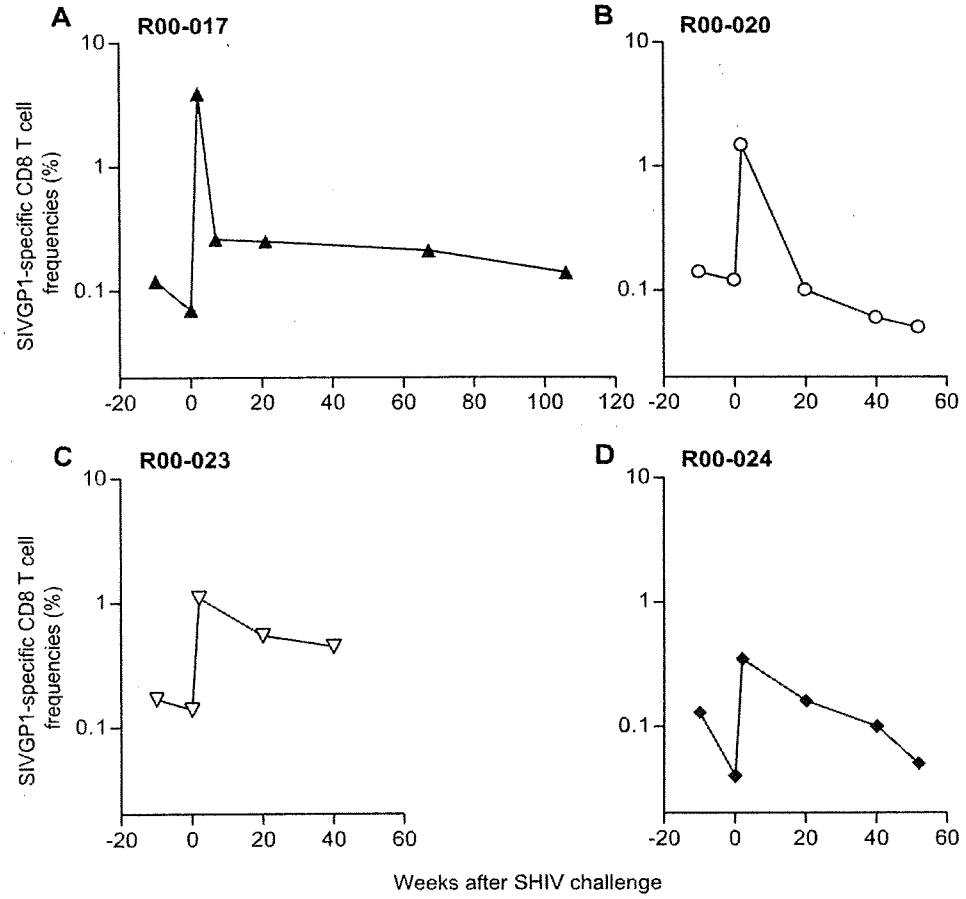

FIG. 3. SIVGP1-specific $CD8^+$ T-cell frequencies in macaques before and after SHIV89.6PD challenge. Frequencies of $CD8^+$ T cells showing SIVGP1-specific IFN-γ induction per total $CD8^+$ T cells in PBMCs are shown. The first time point prechallenge is 10 weeks before challenge.

CD20 depletion and SIVmac239 superchallenge in the SHIV controllers. Macaques R00-017 and R00-020 were further followed up and received monoclonal anti-CD20 antibody administration at week 166 (R00-017) or week 140 (R00-020) and SIVmac239 superchallenge at week 203 (R00-017) or week 151 (R00-020) (Table 1). Viral control was not abrogated, and plasma viremia remained undetectable after anti-CD20 antibody administration (Fig. 4). In both macaques, SHIV89.6PD-specific neutralizing antibodies (NAbs) were induced efficiently after SHIV89.6PD challenge and maintained at high levels in the chronic phase (54). The monoclonal anti-CD20 antibody administration resulted in rapid and prolonged depletion of peripheral $CD20^+$ lymphocytes, and more than a few months later, an approximately fourfold reduction in SHIV-specific NAb levels was observed (Fig. 5).

The following SIVmac239 superchallenge was contained in both macaques (Fig. 4). Macaque R00-017 did not show detectable plasma viremia even after SIVmac239 superchallenge, and macaque R00-020 showed only transient appearance of plasma viremia 1 week after SIVmac239 superchallenge. SIVmac239 *env* RNA but not SHIV89.6PD *env* RNA was detected in the transient plasma viremia (Fig. 6). SIVGP1-specific $CD8^+$ T-cell frequencies were at marginal levels just

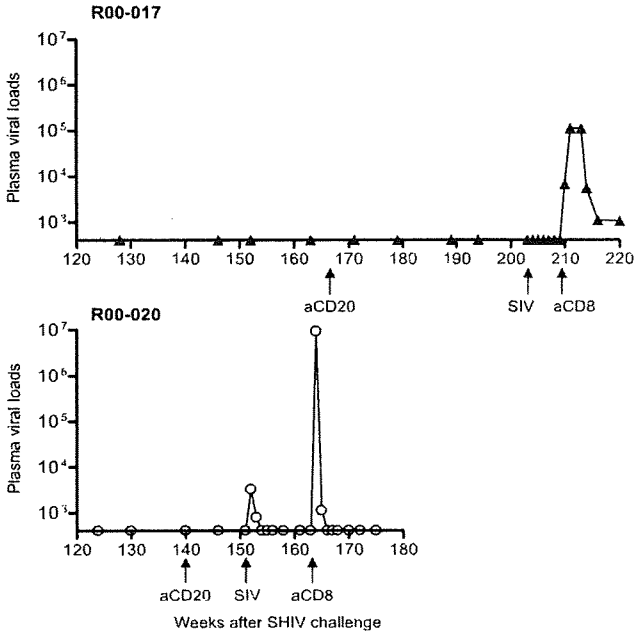

FIG. 4. Plasma viral loads (SIV *gag* RNA copies/ml plasma) in macaques R00-017 (upper panel) and R00-020 (lower panel) after week 120 post-SHIV challenge. aCD20 and aCD8, anti-CD20 and anti-CD8, respectively.

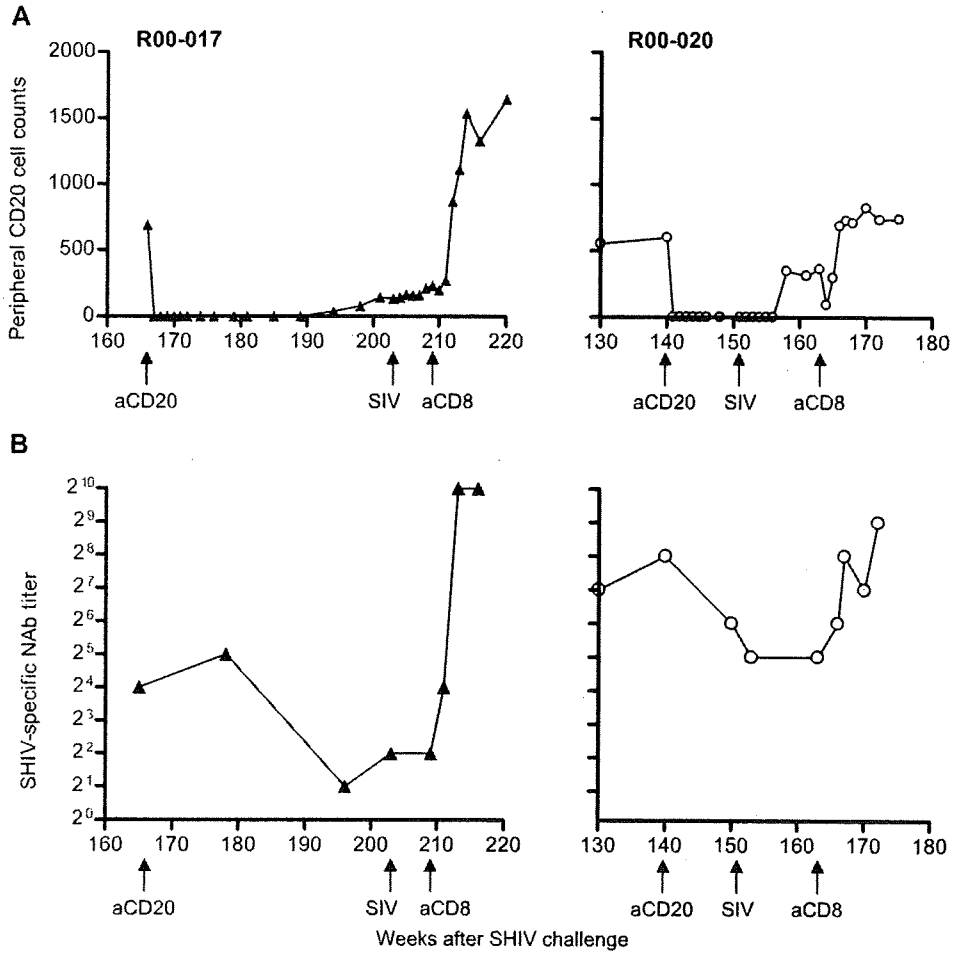

FIG. 5. Changes in SHIV89.6PD-specific NAb levels after monoclonal anti-CD20 antibody administration at week 166 in macaque R00-017 (left panels) and at week 140 in macaque R00-020 (right panels). (A) Peripheral $CD20^+$ cell counts (per μl). (B) SHIV89.6PD-specific neutralizing titers in plasma. aCD20 and aCD8, anti-CD20 and anti-CD8, respectively.

before SIVmac239 superchallenge but increased after the superchallenge (Fig. 7).

CD8 depletion after SIVmac239 superchallenge. Macaques R00-017 and R00-020 received monoclonal anti-CD8 antibody administration at week 209 (6 weeks after superchallenge) and week 163 (12 weeks after superchallenge), respectively (Table 1). Both macaques showed transient depletion of peripheral $CD8^+$ T lymphocytes and appearance of plasma viremia after the anti-CD8 antibody administration (Fig. 6).

In macaque R00-020, exhibiting a shorter period of $CD8^+$ T-lymphocyte depletion, plasma viremia was transient and detectable only at weeks 164 and 165, 1 and 2 weeks after the initial anti-CD8 antibody treatment. SIVmac239 *env* RNA but not SHIV89.6PD *env* RNA was detected in the transient plasma viremia. In macaque R00-017, exhibiting a longer period of $CD8^+$ T-lymphocyte depletion, plasma viremia appeared at week 210, 1 week after the initial anti-CD8 antibody treatment, and remained detectable during the observation period of 3 months. Interestingly, both SIVmac239 *env* RNA and SHIV89.6PD *env* RNA were detected; the former became detectable at week 210 and was detected during the observation period, whereas the latter was detected only at weeks 211 and 212. The former SIVmac239 *env* RNA levels peaked at week 213, and the latter SHIV89.6PD *env* RNA levels peaked at week 211.

SIVmac239-specific NAb responses were undetectable even after SIVmac239 superchallenge and CD8 depletion in both of the macaques (data not shown). SHIV89.6PD-specific NAb titers increased after the CD8 depletion not only in macaque R00-017 showing SHIV89.6PD viremia but also in macaque R00-020 without SHIV89.6PD viremia (Fig. 5). Both macaques showed increases in SIVGP1-specific $CD8^+$ T-cell frequencies after recovery from peripheral $CD8^+$ T-lymphocyte depletion (Fig. 7).

DISCUSSION

Previous $CD8^+$ cell depletion experiments in macaques using a monoclonal anti-CD8 antibody have indicated the importance of $CD8^+$ cell responses in SIV control in vivo (12, 29, 42). The present study evaluated the anti-SIV efficacy of these bulk $CD8^+$ cells in the vaccinated macaques that exhibited prophylactic SeV-Gag vaccine-based control of viral replication and showed induction of $CD8^+$ cells able to efficiently

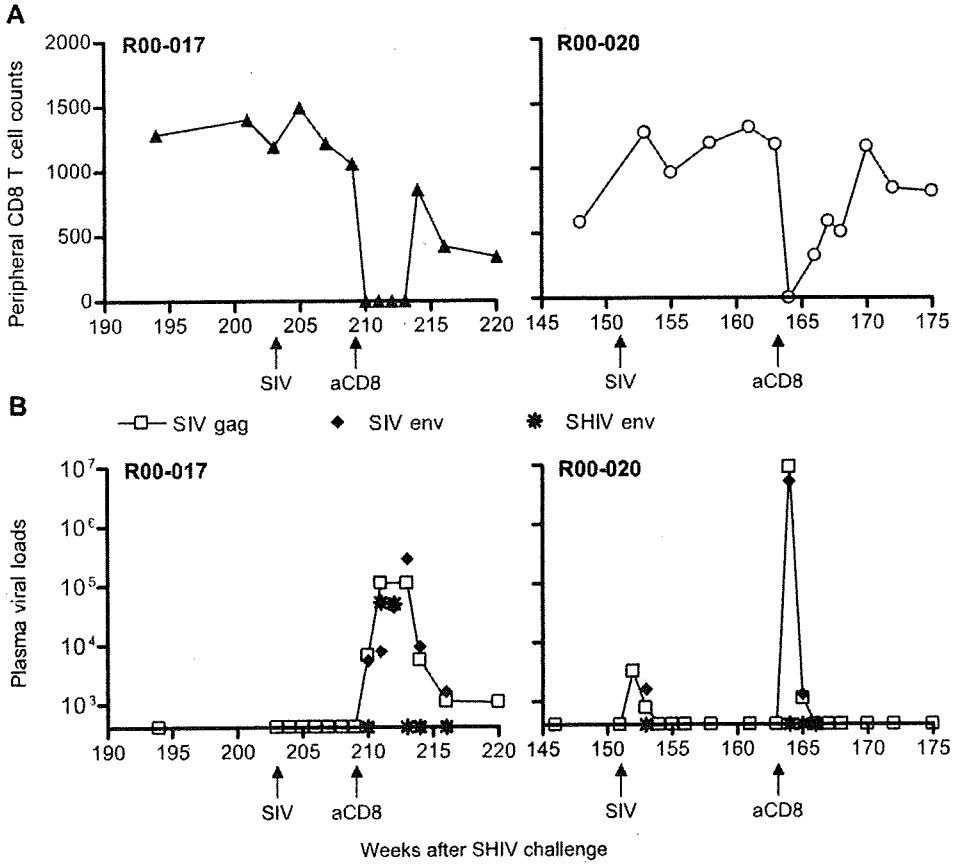

FIG. 6. SIVmac239 superchallenge and $CD8^+$ cell depletion in macaques R00-017 and R00-020. Macaque R00-017 received SIVmac239 superchallenge at week 203 and monoclonal anti-CD8 (aCD8) antibody administration starting at week 209, while macaque R00-020 received superchallenge at week 151 and anti-CD8 at week 163. (A) Peripheral $CD8^+$ T-cell counts (per μl) in macaques R00-017 (left panel) and R00-020 (right panel). (B) Plasma viral loads (copies/ml plasma) in macaques R00-017 (left panel) and R00-020 (right panel). In addition to SIV *gag* RNA levels, levels of SIV *env* RNA and SHIV *env* RNA at several time points are shown.

suppress SIV replication in vitro after SHIV challenge in these macaques. The difference in anti-SIV efficacies between postvaccination/prechallenge and postchallenge $CD8^+$ cells may explain why protective immune responses can be consistently induced not by current viral vector vaccination but by live virus infection.

These bulk $CD8^+$ cells are considered to include $CD8^+$ NK cells in addition to $CD8^+$ T lymphocytes. While previous studies using bulk $CD8^+$ cells or CTL clones (9, 24, 48, 55) have shown the importance of CTL activity on suppression of HIV/SIV replication, there may be a possibility that NK cells exert some suppressive effect on SIV replication, contributing to reductions in SIV production by prevaccination $CD8^+$ cells in the present study. The suppressive effect of postvaccination/prechallenge $CD8^+$ cells was not larger than that of prevaccination except for macaque R00-020. In contrast, postchallenge $CD8^+$ cells suppressed SIV replication more efficiently than those prevaccination and postvaccination. In the in vitro assay of SIV replication, individual macaques showed different sensitivities of target $CD8^-$ cells to SIV infection and different patterns of SIV replication kinetics in the absence of $CD8^+$ cells (Fig. 1). In macaque R00-023 showing higher levels of SIV production in the absence of $CD8^+$ cells, SIV infection at a lower MOI might exhibit a larger reduction in SIV production by addition of postchallenge $CD8^+$ cells.

Gag-specific $CD8^+$ T-cell levels peaked around 1 week after SeV-Gag vaccination and then decreased in the late phase after that (28). To prepare postvaccination/prechallenge $CD8^+$ cells, we used PBMCs in the late phase without those at week 1 post-SeV-Gag vaccination that include the peak levels of Gag-specific $CD8^+$ T cells. Thus, we compared anti-SIV efficacy of $CD8^+$ cells in the late phase postvaccination with that in the chronic phase post-SHIV challenge in this study. The postvaccination/prechallenge SIVGP1-specific $CD8^+$ T-cell frequencies roughly reflect Gag-specific $CD8^+$ T-cell ones because SIVGP1-specific $CD8^+$ T-cell responses were undetectable before SeV-Gag vaccination (data not shown). On the other hand, the postchallenge SIVGP1-specific $CD8^+$ T-cell responses are considered specific for SHIV antigens, including SIV-derived Gag, Pol, Vif, and partial Vpr. Therefore, our results shown in Fig. 3 suggest that SIV-specific $CD8^+$ T-cell frequencies in the chronic phase post-SHIV challenge were less than those post-SeV-Gag vaccination (prechallenge) in macaque R00-020. Interestingly, however, such postchallenge $CD8^+$ cells suppressed SIV replication more efficiently than postvaccination/prechallenge ones. Thus, SIV-specific $CD8^+$

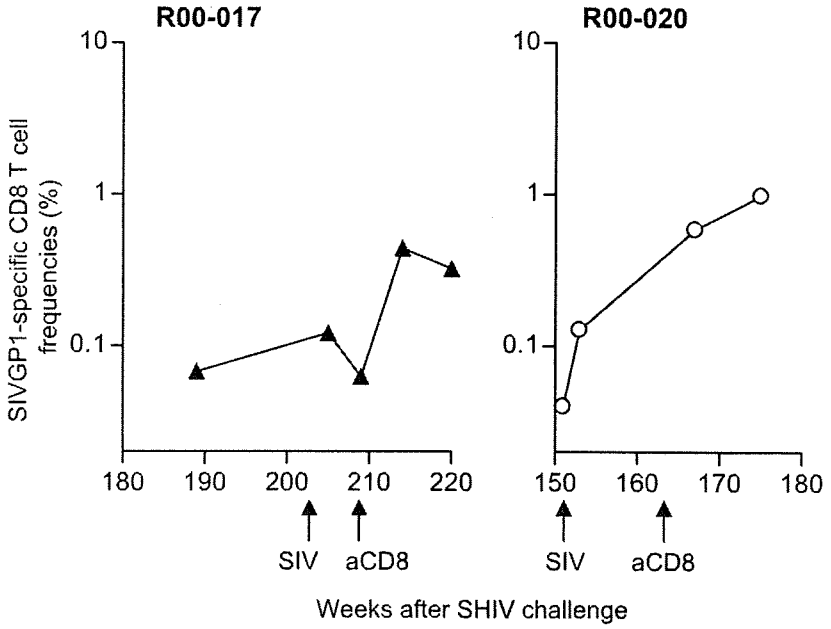

FIG. 7. SIVGP1-specific $CD8^-$ T-cell frequencies in macaques R00-017 (left panel) and R00-020 (right panel) before and after SIVmac239 superchallenge. Frequencies of $CD8^-$ T cells showing SIVGP1-specific IFN-γ induction per total $CD8^+$ T cells in PBMCs are shown. aCD8, anti-CD8.

T-cell frequencies may not always correlate with anti-SIV efficacy in vitro. It may be because postchallenge-induced, certain epitope-specific $CD8^+$ T cells may have higher anti-SIV efficacy in vitro than postvaccination/prechallenge $CD8^+$ T cells in this macaque. There may be a possibility of augmentation of anti-SIV efficacy by induction of broader $CD8^+$ T-cell responses after SHIV challenge.

A previous $CD8^+$ cell depletion study in macaques infected with live attenuated SIV has shown partial loss of superchallenged SIVmac251 control by monoclonal anti-CD8 antibody administration at the superchallenge and has suggested involvement of both cellular and humoral immune responses in this control (43). On the other hand, administration of monoclonal anti-CD8 antibody to macaques infected with live attenuated SIVmac239Δnef after SIVmac251 superchallenge resulted in the appearance of SIVmac239Δnef viremia without detectable SIVmac251 viremia (33). In contrast, the present study showed the appearance of superchallenged SIVmac239 viremia by monoclonal anti-CD8 antibody administration after superchallenge, suggesting that $CD8^+$ cells were crucial for the control of superchallenged SIVmac239 replication. It can be speculated that, in SIVmac239Δnef-infected animals, live virus replication levels before superchallenge were higher, resulting in more strict containment of superchallenge than that in our study. Additionally, neutralizing antibody responses may be involved in the containment of superchallenge in SIVmac239Δnef-infected animals but not in SHIV-infected ones. Thus, our results imply a more profound contribution of $CD8^-$ cells to control of SIV superchallenge in the absence of NAb help.

More than a few months after the anti-CD20 antibody administration, both macaques R00-017 and R00-020 showed fourfold reductions in SHIV-specific neutralizing titers, although it is unclear if these reductions were due to the $CD20^+$ cell depletion. Macaque R00-017 with a lower neutralizing titer showed transient appearance of SHIV viremia by $CD8^+$ cell depletion, but macaque R00-020 with a higher titer did not. These results were consistent with the previous study indicating involvement of humoral as well as cellular immune responses in the CXCR4-tropic SHIV control (26).

In summary, our results indicate that $CD8^+$ cells acquired the ability to efficiently suppress CCR5-tropic SIV replication in vitro by controlled CXCR4-tropic SHIV infection. While the levels of in vitro anti-SIV efficacy resulting in SIV control in vivo have not been determined, our results imply that such $CD8^+$ cell responses may be crucial for live attenuated vaccine-based containment of HIV/SIV superinfection.

ACKNOWLEDGMENTS

This work was supported by a grant from the Ministry of Education, Culture, Sports, Science, and Technology; grants from the Japan Health Sciences Foundation; and grants from the Ministry of Health, Labor, and Welfare in Japan.

The animal experiments were conducted through the Cooperative Research Program at the Tsukuba Primate Research Center, National Institute of Biomedical Innovation, with the help of the Corporation for Production and Research of Laboratory Primates. We thank Centocor, Inc., and K. A. Reimann for providing cM-T807 and M. Takiguchi, F. Ono, K. Komatsuzaki, A. Hiyaoka, A. Oyama, K. Oto, H. Akari, K. Terao, M. Miyazawa, A. Kimura, K. Mori, N. Yamamoto, T. Sata, T. Kurata, Y. Nagai, and A. Nomoto for their help.

REFERENCES

1. **Altfeld, M., and E. S. Rosenberg.** 2000. The role of $CD4^+$ T helper cells in the cytotoxic T lymphocyte response to HIV-1. Curr. Opin. Immunol. **12**: 375–380.
2. **Amara, R. R., F. Villinger, J. D. Altman, S. L. Lydy, S. P. O'Neil, S. I. Staprans, D. C. Montefiori, Y. Xu, J. G. Herndon, L. S. Wyatt, M. A.**

Candido, N. L. Kozyr, P. L. Earl, J. M. Smith, H. L. Ma, B. D. Grimm, M. L. Hulsey, J. Miller, H. M. McClure, J. M. McNicholl, B. Moss, and H. L. Robinson. 2001. Control of a mucosal challenge and prevention of AIDS in rhesus macaques by a multiprotein DNA/MVA vaccine. Science **292:**69–74.

3. **Baba, T. W., Y. S. Jeong, D. Pennick, R. Bronson, M. F. Greene, and R. M. Ruprecht.** 1995. Pathogenicity of live, attenuated SIV after mucosal infection of neonatal macaques. Science **267:**1820–1825.
4. **Borrow, P., H. Lewicki, B. H. Hahn, G. M. Shaw, and M. B. A. Oldstone.** 1994. Virus-specific $CD8^+$ cytotoxic T-lymphocyte activity associated with control of viremia in primary human immunodeficiency virus type 1 infection. J. Virol. **68:**6103–6110.
5. **Brander, C., and B. D. Walker.** 1999. T lymphocyte responses in HIV-1 infection: implication for vaccine development. Curr. Opin. Immunol. **11:** 451–459.
6. **Casimiro, D. R., F. Wang, W. A. Schleif, X. Liang, Z.-Q. Zhang, T. W. Tobery, M.-E. Davies, A. B. McDermott, D. H. O'Connor, A. Fridman, A. Bagchi, L. G. Tussey, A. J. Bett, A. C. Finnefrock, T.-M. Fu, A. Tang, K. A. Wilson, M. Chen, H. C. Perry, G. J. Heidecker, D. C. Freed, A. Carella, K. S. Punt, K. J. Sykes, L. Huang, V. I. Ausensi, M. Bachinsky, U. Sadasivan-Nair, D. I. Watkins, E. A. Emini, and J. W. Shiver.** 2005. Attenuation of simian immunodeficiency virus SIVmac239 infection by prophylactic immunization with DNA and recombinant adenoviral vaccine vectors expressing Gag. J. Virol. **79:**15547–15555.
7. **Daniel, M. D., F. Kirchhoff, S. C. Czajak, P. K. Sehgal, and R. C. Desrosiers.** 1992. Protective effects of a live attenuated SIV vaccine with a deletion in the nef gene. Science **258:**1938–1941.
8. **Feinberg, M. B., and J. P. Moore.** 2002. AIDS vaccine models: challenging challenge viruses. Nat. Med. **8:**207–210.
9. **Gauduin, M.-C., R. L. Glickman, R. Means, and R. P. Johnson.** 1998. Inhibition of simian immunodeficiency virus (SIV) replication by $CD8^+$ T lymphocytes from macaques immunized with live attenuated SIV. J. Virol. **72:**6315–6324.
10. **Goulder, P. J., and D. I. Watkins.** 2004. HIV and SIV CTL escape: implications for vaccine design. Nat. Rev. Immunol. **4:**630–640.
11. **Horton, H., T. U. Vogel, D. K. Carter, K. Vielhuber, D. H. Fuller, T. Shipley, J. T. Fuller, K. J. Kunstman, G. Sutter, D. C. Montefiori, V. Erfle, R. C. Desrosiers, N. Wilson, L. J. Picker, S. M. Wolinsky, C. Wang, D. B. Allison, and D. I. Watkins.** 2002. Immunization of rhesus macaques with a DNA prime/modified vaccinia virus Ankara boost regimen induces broad simian immunodeficiency virus (SIV)-specific T-cell responses and reduces initial viral replication but does not prevent disease progression following challenge with pathogenic SIVmac239. J. Virol. **76:**7187–7202.
12. **Jin, X., D. E. Bauer, S. E. Tuttleton, S. Lewin, A. Gettie, J. Blanchard, C. E. Irwin, J. T. Safrit, J. Mittler, L. Weinberger, L. G. Kostrikis, L. Zhang, A. S. Perelson, and D. D. Ho.** 1999. Dramatic rise in plasma viremia after CD8+ T cell depletion in simian immunodeficiency virus-infected macaques. J. Exp. Med. **189:**991–998.
13. **Johnson, R. P., and R. C. Desrosiers.** 1998. Protective immunity induced by live attenuated simian immunodeficiency virus. Curr. Opin. Immunol. **10:** 436–443.
14. **Johnson, R. P., J. D. Lifson, S. C. Czajak, K. S. Cole, K. H. Manson, R. Glickman, J. Yang, D. C. Montefiori, R. Montelaro, M. S. Wyand, and R. C. Desrosiers.** 1999. Highly attenuated vaccine strains of simian immunodeficiency virus protect against vaginal challenge: inverse relationship of degree of protection with level of attenuation. J. Virol. **73:**4952–4961.
15. **Kano, M., T. Matano, A. Kato, H. Nakamura, A. Takeda, Y. Suzaki, Y. Ami, K. Terao, and Y. Nagai.** 2002. Primary replication of a recombinant Sendai virus vector in macaques. J. Gen. Virol. **83:**1377–1386.
16. **Kato, A., Y. Sakai, T. Shioda, T. Kondo, M. Nakanishi, and Y. Nagai.** 1996. Initiation of Sendai virus multiplication from transfected cDNA or RNA with negative or positive sense. Genes Cells **1:**569–579.
17. **Kawada, M., T. Tsukamoto, H. Yamamoto, A. Takeda, H. Igarashi, D. I. Watkins, and T. Matano.** 2007. Long-term control of simian immunodeficiency virus replication with central memory $CD4^+$ T-cell preservation after nonsterile protection by a cytotoxic T-lymphocyte-based vaccine. J. Virol. **81:**5202–5211.
18. **Kestler, H. W., III, D. J. Ringler, K. Mori, D. L. Panicali, P. K. Sehgal, M. D. Daniel, and R. C. Desrosiers.** 1991. Importance of the nef gene for maintenance of high virus loads and for development of AIDS. Cell **65:**651–662.
19. **Koff, W. C., P. R. Johnson, D. I. Watkins, D. R. Burton, J. D. Lifson, K. J. Hasenkrug, A. B. McDermott, A. Schultz, T. J. Zamb, R. Boyle, and R. C. Desrosiers.** 2006. HIV vaccine design: insights from live attenuated SIV vaccines. Nat. Immunol. **7:**19–23.
20. **Koup, R. A., J. T. Safrit, Y. Cao, C. A. Andrews, G. McLeod, W. Borkowsky, C. Farthing, and D. D. Ho.** 1994. Temporal association of cellular immune responses with the initial control of viremia in primary human immunodeficiency virus type 1 syndrome. J. Virol. **68:**4650–4655.
21. **Letvin, N. L., J. R. Mascola, Y. Sun, D. A. Gorgone, A. P. Buzby, L. Xu, Z. Y. Yang, B. Chakrabarti, S. S. Rao, J. E. Schmitz, D. C. Montefiori, B. R. Barker, F. L. Bookstein, and G. J. Nabel.** 2006. Preserved $CD4^+$ central memory T cells and survival in vaccinated SIV-challenged monkeys. Science **312:**1530–1533.
22. **Li, H.-O., Y.-F. Zhu, M. Asakawa, H. Kuma, T. Hirata, Y. Ueda, Y.-S. Lee, M. Fukumura, A. Iida, A. Kato, Y. Nagai, and M. Hasegawa.** 2000. A cytoplasmic RNA vector derived from nontransmissible Sendai virus with efficient gene transfer and expression. J. Virol. **74:**6564–6569.
23. **Li, Q., L. Duan, J. D. Estes, Z. M. Ma, T. Rourke, Y. Wang, C. Reilly, J. Carlis, C. J. Miller, and A. T. Haase.** 2005. Peak SIV replication in resting memory $CD4^+$ T cells depletes gut lamina propria $CD4^+$ T cells. Nature **434:**1148–1152.
24. **Loffredo, J. T., E. G. Rakasz, J. P. Giraldo, S. P. Spencer, K. K. Grafton, S. R. Martin, G. Napoé, L. J. Yant, N. A. Wilson, and D. I. Watkins.** 2005. $Tat_{28-35}SL8$-specific $CD8^+$ T lymphocytes are more effective than $Gag_{181-189}CM9$-specific $CD8^+$ T lymphocytes at suppressing simian immunodeficiency virus replication in a functional in vitro assay. J. Virol. **79:**14986–14991.
25. **Lu, Y., C. D. Pauza, X. Lu, D. C. Montefiori, and C. J. Miller.** 1998. Rhesus macaques that become systemically infected with pathogenic SHIV 89.6-PD after intravenous, rectal, or vaginal inoculation and fail to make an antiviral antibody response rapidly develop AIDS. J. Acquir. Immune Defic. Syndr. Hum. Retrovirol. **19:**6–18.
26. **Mao, H., B. A. P. Lafont, T. Igarashi, Y. Nishimura, C. Brown, V. Hirsch, A. Buckler-White, R. Sadjadpour, and M. A. Martin.** 2005. $CD8^+$ and $CD20^+$ lymphocytes cooperate to control acute simian immunodeficiency virus/human immunodeficiency virus chimeric virus infections in rhesus monkeys: modulation by major histocompatibility complex genotype. J. Virol. **79:**14887–14898.
27. **Matano, T., M. Kano, H. Nakamura, A. Takeda, and Y. Nagai.** 2001. Rapid appearance of secondary immune responses and protection from acute CD4 depletion after a highly pathogenic immunodeficiency virus challenge in macaques vaccinated with a DNA prime/Sendai viral vector boost regimen. J. Virol. **75:**11891–11896.
28. **Matano, T., M. Kobayashi, H. Igarashi, A. Takeda, H. Nakamura, M. Kano, C. Sugimoto, K. Mori, A. Iida, T. Hirata, M. Hasegawa, T. Yuasa, M. Miyazawa, Y. Takahashi, M. Yasunami, A. Kimura, D. H. O'Connor, D. I. Watkins, and Y. Nagai.** 2004. Cytotoxic T lymphocyte-based control of simian immunodeficiency virus replication in a preclinical AIDS vaccine trial. J. Exp. Med. **199:**1709–1718.
29. **Matano, T., R. Shibata, C. Siemon, M. Connors, H. C. Lane, and M. A. Martin.** 1998. Administration of an anti-CD8 monoclonal antibody interferes with the clearance of chimeric simian/human immunodeficiency virus during primary infections of rhesus macaques. J. Virol. **72:**164–169.
30. **Mattapallil, J. J., D. C. Douek, A. Buckler-White, D. C. Montefiori, N. L. Letvin, G. J. Nabel, and M. Roederer.** 2006. Vaccination preserves CD4 memory T cells during acute simian immunodeficiency virus challenge. J. Exp. Med. **203:**1533–1541.
31. **Mattapallil, J. J., D. C. Douek, B. Hill, Y. Nishimura, M. A. Martin, and M. Roederer.** 2005. Massive infection and loss of memory $CD4^+$ T cells in multiple tissues during acute SIV infection. Nature **434:**1093–1097.
32. **McMichael, A. J., and T. Hanke.** 2003. HIV vaccines 1983–2003. Nat. Med. **9:**874–880.
33. **Metzner, K. J., X. Jin, F. V. Lee, A. Gettie, D. E. Bauer, M. D. Mascio, A. S. Perelson, P. A. Marx, D. D. Ho, L. G. Kostrikis, and R. I. Connor.** 1999. Effects of in vivo CD8+ T cell depletion on virus replication in rhesus macaques immunized with a live, attenuated simian immunodeficiency virus vaccine. J. Exp. Med. **191:**1921–1932.
34. **Miller, C. J., and K. Abel.** 2005. Immune mechanisms associated with protection from vaginal SIV challenge in rhesus monkeys infected with virulence-attenuated SHIV 89.6. J. Med. Primatol. **34:**271–281.
35. **Miller, C. J., M. B. McChesney, X. Lü, P. J. Dailey, C. Chutkowski, D. Lu, P. Brosio, B. Roberts, and Y. Lu.** 1997. Rhesus macaques previously infected with simian/human immunodeficiency virus are protected from vaginal challenge with pathogenic SIVmac239. J. Virol. **71:**1911–1921.

35a. **National Institute of Infectious Diseases.** 2007. Guides for animal experiments performed at National Institute of Infectious Diseases. National Institute of Infectious Diseases, Tokyo, Japan. (In Japanese).

36. **Nishimura, Y., C. R. Brown, J. J. Mattapallil, T. Igarashi, A. Buckler-White, B. A. Lafont, V. M. Hirsch, M. Roederer, and M. A. Martin.** 2005. Resting naive $CD4^+$ T cells are massively infected and eliminated by X4-tropic simian-human immunodeficiency viruses in macaques. Proc. Natl. Acad. Sci. USA **102:**8000–8005.
37. **Nishimura, Y., T. Igarashi, O. K. Donau, A. Buckler-White, C. Buckler, B. A. Lafont, R. M. Goeken, S. Goldstein, V. M. Hirsch, and M. A. Martin.** 2004. Highly pathogenic SHIVs and SIVs target different $CD4^+$ T cell subsets in rhesus monkeys, explaining their divergent clinical courses. Proc. Natl. Acad. Sci. USA **101:**12324–12329.
38. **Ogg, G. S., X. Jin, S. Bonhoeffer, P. R. Dunbar, M. A. Nowak, S. Monard, J. P. Segal, Y. Cao, S. L. Rowland-Jones, V. Cerundolo, A. Hurley, M. Markowitz, D. D. Ho, D. F. Nixon, and A. J. McMichael.** 1998. Quantitation of HIV-1-specific cytotoxic T lymphocytes and plasma load of viral RNA. Science **279:**2103–2106.
39. **Picker, L. J., and D. I. Watkins.** 2005. HIV pathogenesis: the first cut is the deepest. Nat. Immunol. **6:**430–432.
40. **Rose, N. F., P. A. Marx, A. Luckay, D. F. Nixon, W. J. Moretto, S. M. Donahoe, D. Montefiori, A. Roberts, L. Buonocore, and J. K. Rose.** 2001. An

effective AIDS vaccine based on live attenuated vesicular stomatitis virus recombinants. Cell **106**:539–549.
41. **Rosenberg, E. S., J. M. Billingsley, A. M. Caliendo, S. L. Boswell, P. E. Sax, S. A. Kalams, and B. D. Walker.** 1997. Vigorous HIV-1-specific CD4+ T cell responses associated with control of viremia. Science **278**:1447–1450.
42. **Schmitz, J. E., M. J. Kuroda, S. Santra, V. G. Sasseville, M. A. Simon, M. A. Lifton, P. Racz, K. Tenner-Racz, M. Dalesandro, B. J. Scallon, J. Ghrayeb, M. A. Forman, D. C. Montefiori, E. P. Rieber, N. L. Letvin, and K. A. Reimann.** 1999. Control of viremia in simian immunodeficiency virus infection by CD8+ lymphocytes. Science **283**:857–860.
43. **Schmitz, J. E., R. P. Johnson, H. M. McClure, K. H. Manson, M. S. Wyand, M. J. Kuroda, M. A. Lifton, R. S. Khunkhun, K. J. McEvers, J. Gillis, M. Piatak, J. D. Lifson, G. Grosschupff, P. Racz, K. Tenner-Racz, E. P. Rieber, K. Kuus-Reichel, R. S. Gelman, N. L. Letvin, D. C. Montefiori, R. M. Ruprecht, R. C. Desrosiers, and K. A. Reimann.** 2005. Effect of CD8+ lymphocyte depletion on virus containment after simian immunodeficiency virus SIVmac251 challenge of live attenuated SIVmac239Δ3-vaccinated rhesus macaques. J. Virol. **79**:8131–8141.
44. **Shibata, R., C. Siemon, S. C. Czajak, R. C. Desrosiers, and M. A. Martin.** 1997. Live, attenuated simian immunodeficiency virus vaccines elicit potent resistance against a challenge with a human immunodeficiency virus type 1 chimeric virus. J. Virol. **71**:8141–8148.
45. **Shibata, R., F. Maldarelli, C. Siemon, T. Matano, M. Parta, G. Miller, T. Fredrickson, and M. A. Martin.** 1997. Infection and pathogenicity of chimeric simian-human immunodeficiency viruses in macaques: determinants of high virus loads and CD4 cell killing. J. Infect. Dis. **176**:362–373.
46. **Shiver, J. W., T. M. Fu, L. Chen, D. R. Casimiro, M. E. Davies, R. K. Evans, Z. Q. Zhang, A. J. Simon, W. L. Trigona, S. A. Dubey, L. Huang, V. A. Harris, R. S. Long, X. Liang, L. Handt, W. A. Schleif, L. Zhu, D. C. Freed, N. V. Persaud, L. Guan, K. S. Punt, A. Tang, M. Chen, K. A. Wilson, K. B. Collins, G. J. Heidecker, V. R. Fernandez, H. C. Perry, J. G. Joyce, K. M. Grimm, J. C. Cook, P. M. Keller, D. S. Kresock, H. Mach, R. D. Troutman, L. A. Isopi, D. M. Williams, Z. Xu, K. E. Bohannon, D. B. Volkin, D. C. Montefiori, A. Miura, G. R. Krivulka, M. A. Lifton, M. J. Kuroda, J. E. Schmitz, N. L. Letvin, M. J. Caulfield, A. J. Bett, R. Youil, D. C. Kaslow, and E. A. Emini.** 2002. Replication-incompetent adenoviral vaccine vector elicits effective anti-immunodeficiency-virus immunity. Nature **415**:331–335.
47. **Takeda, A., H. Igarashi, H. Nakamura, M. Kano, A. Iida, T. Hirata, M. Hasegawa, Y. Nagai, and T. Matano.** 2003. Protective efficacy of an AIDS vaccine, a single DNA priming followed by a single booster with a recombinant replication-defective Sendai virus vector, in a macaque AIDS model. J. Virol. **77**:9710–9715.
48. **Tomiyama, H., M. Fujiwara, S. Oka, and M. Takiguchi.** 2005. Epitope-dependent effect of Nef-mediated HLA class I down-regulation on ability of HIV-1-specific CTLs to suppress HIV-1 replication. J. Immunol. **174**:36–40.
49. **Veazey, R. S., K. G. Mansfield, I. C. Tham, A. C. Carville, D. E. Shvetz, A. E. Forand, and A. A. Lackner.** 2000. Dynamics of CCR5 expression by CD4+ T cells in lymphoid tissues during simian immunodeficiency virus infection. J. Virol. **74**:11001–11007.
50. **Veazey, R. S., M. DeMaria, L. V. Chalifoux, D. E. Shvetz, D. R. Pauley, H. L. Knight, M. Rosenzweig, R. P. Johnson, R. C. Desrosiers, and A. A. Lackner.** 1998. Gastrointestinal tract as a major site of CD4+ T cell depletion and viral replication in SIV infection. Science **280**:427–431.
51. **Voss, G., S. Nick, C. Stahl-Hennig, K. Ritter, and G. Hunsmann.** 1992. Generation of macaque B lymphoblastoid cell lines with simian Epstein-Barr-like viruses: transformation procedure, characterization of the cell lines and occurrence of simian foamy virus. J. Virol. Methods **39**:185–195.
52. **Wilson, N. A., J. Reed, G. S. Napoe, S. Piaskowski, A. Szymanski, J. Furlott, E. J. Gonzalez, L. J. Yant, N. J. Maness, G. E. May, T. Soma, M. R. Reynolds, E. Rakasz, R. Rudersdorf, A. B. McDermott, D. H. O'Connor, T. C. Friedrich, D. B. Allison, A. Patki, L. J. Picker, D. R. Burton, J. Lin, L. Huang, D. Patel, G. Heindecker, J. Fan, M. Citron, M. Horton, F. Wang, X. Liang, J. W. Shiver, D. R. Casimiro, and D. I. Watkins.** 2006. Vaccine-induced cellular immune responses reduce plasma viral concentrations after repeated low-dose challenge with pathogenic simian immunodeficiency virus SIVmac239. J. Virol. **80**:5875–5885.
53. **Wyand, M. S., K. H. Manson, M. Garcia-Moll, D. C. Montefiori, and R. C. Desrosiers.** 1996. Vaccine protection by a triple deletion mutant of simian immunodeficiency virus. J. Virol. **70**:3724–3733.
54. **Yamamoto, H., M. Kawada, T. Tsukamoto, A. Takeda, H. Igarashi, M. Miyazawa, T. Naruse, M. Yasunami, A. Kimura, and T. Matano.** 2007. Vaccine-based, long-term, stable control of simian/human immunodeficiency virus 89.6PD replication in rhesus macaques. J. Gen. Virol. **88**:652–659.
55. **Yang, O. O., S. A. Kalams, A. Trocha, H. Cao, A. Luster, R. P. Johnson, and B. D. Walker.** 1997. Suppression of human immunodeficiency virus type 1 replication by CD8+ cells: evidence for HLA class I-restricted triggering of cytolytic and noncytolytic mechanisms. J. Virol. **71**:3120–3128.

ELSEVIER

INSTITUT PASTEUR

Microbes and Infection 9 (2007) 1590–1596

www.elsevier.com/locate/micinf

Original article

Inhibition of infectious murine leukemia virus production by *Fv-4 env* gene products exerting dominant negative effect on viral envelope glycoprotein

Akiko Takeda [a], Tetsuro Matano [a,b,*]

[a] *International Research Center for Infectious Diseases, The Institute of Medical Science, The University of Tokyo, 4-6-1 Shirokanedai, Minato-ku, Tokyo 108-8639, Japan*

[b] *AIDS Research Center, National Institute of Infectious Diseases, 1-23-1 Toyama, Shinjuku-ku, Tokyo 162-8640, Japan*

Received 5 August 2007; accepted 9 September 2007

Available online 23 September 2007

Abstract

Fv-4 is a mouse gene that confers resistance against ecotropic murine leukemia virus (MLV) infection on mice. While receptor interference by the *Fv-4 env* gene product, Fv-4 Env, that can bind to the ecotropic MLV receptor has been shown to play an important role in the resistance, other mechanisms have also been suggested because it confers extremely efficient, complete resistance in vivo. Here, we have examined the effect of Fv-4 Env on infectious MLV production. Infectious MLV titers in supernatants obtained after transfection with a Friend MLV (FMLV) Env-expressing plasmid from MLV *gag–pol* producer cells harboring a retroviral vector were largely reduced by coexpression of Fv-4 Env. Syncytia formation mediated by R-peptide-deleted FMLV Env in NIH 3T3 cells was impaired by Fv-4 Env coexpression. Similarly, Fv-4 Env inhibited infectious amphotropic MLV production and syncytia formation mediated by R-peptide-deleted amphotropic MLV Env. Immunoprecipitation analysis revealed interaction of Fv-4 Env with amphotropic MLV Env as well as FMLV Env. These results indicate that Fv-4 Env inhibits infectious ecotropic and amphotropic MLV production by exerting dominant negative effect on MLV Env, suggesting contribution of this inhibitory effect to the resistance against ecotropic MLV infection in *Fv-4*-expressing mice.

Keywords: MLV; Fv-4; Env

1. Introduction

The *Fv-4* locus has been identified as a dominant gene that confers resistance to Friend virus-induced disease in mice [1]. *Fv-4* corresponds to a defective endogenous provirus with an ecotropic murine leukemia virus (MLV)-like *env* gene [2,3]. The *Fv-4 env* gene product, Fv-4 Env, having approximately 70% amino acid sequence homology with ecotropic Moloney MLV (MoMLV) and Friend MLV (FMLV) Envs has been shown to bind to the ecotropic MLV receptor and inhibit entry of ecotropic MLV into the cells [2,4]. Such receptor interference has been indicated to play an important role in the resistance to Friend virus infection [2]. While contribution of immune responses to this resistance has also been indicated, additional mechanisms have been suggested because *Fv-4* confers extremely efficient, complete resistance in vivo [5–10]. Elucidation of such natural resistance mechanism may lead to development of a strategy against viral infection.

MLVs are divided into several groups such as ecotropic, amphotropic, and xenotropic MLVs according to their receptor usage [11]. The receptor-binding domain locates in the amino (N)-terminal half of Env SU (surface subunit) [12–15]. MLV Envs are oligomerized to form trimers in the endoplasmic reticulum, processed into SU and TM (transmembrane subunit)

* Corresponding author. International Research Center for Infectious Diseases, The Institute of Medical Science, The University of Tokyo, 4-6-1 Shirokanedai, Minato-ku, Tokyo 108-8639, Japan. Tel.: +81 3 6409 2078; fax: +81 3 6409 2076.

E-mail address: matano@m.u-tokyo.ac.jp (T. Matano).

1286-4579/$ - see front matter © 2007 Elsevier Masson SAS. All rights reserved.
doi:10.1016/j.micinf.2007.09.012

in the Golgi apparatus, expressed on the cell surface, and incorporated into the virion [11,16]. MLV Env TM (p15E) is cleaved into p12E and the C-terminal 16-amino-acid long R-peptide at the time of virus budding or shortly thereafter [17]. The R-deleted ecotropic MLV Env induces syncytia in NIH 3T3 cells whereas the wild-type Env does not [18,19].

Previous in vitro studies have shown incomplete inhibition of ecotropic MLV entry in Fv-4 Env-expressing cells [5,6]. This leakage of receptor interference may result in infectious MLV production from the ecotropic MLV-infected cells expressing Fv-4 Env. In the present study, we have examined the effect of Fv-4 Env expression on infectious MLV production from MLV producer cells. Our results showed inhibition of infectious MLV production by Fv-4 Env interacting with the wild-type MLV Env, suggesting contribution of this dominant negative effect to the resistance against ecotropic MLV infection in *Fv-4*-expressing mice.

2. Materials and methods

2.1. DNAs

An ecotropic MLV *env* gene fragment (GenBank accession number X02794 [20]) encoding the wild-type FMLV Env, FE, and an amphotropic MLV *env* gene fragment (GenBank accession number M33469 [21]) encoding the wild-type 4070A Env, AE, were introduced into an expression plasmid, pCXN2 [22], to obtain pCXN2FE and pCXN2AE, respectively. A mutant FMLV Env, FE.D86K [23] (Fig. 1), in which the 86th aspartic acid in FMLV receptor-binding domain was replaced by lysine is equivalent to a previously-reported binding-deficient MoMLV Env mutant, D84K [24]. Like the previously-reported postbinding fusion-defective MoMLV Env whose 461st tyrosine is substituted to proline [25], the 470th tyrosine in FMLV Env and the 455th tyrosine in 4070A Env, equivalent to the 461st tyrosine in MoMLV Env, were replaced by histidine and proline to obtain Env mutants, FE.T470H [23] and AE.T455P, respectively (Fig. 1). The cDNAs encoding the R-deleted FE, R(−)FE, and the R-deleted AE, R(−)AE, were obtained by inserting TAG-stop codon next to the 625th leucine codon in FE and the 610th leucine codon in AE, respectively [23]. An FMLV *env* and a 4070A *env* gene fragments without the stop codon were tagged in frame with an *lck* gene fragment encoding an N-terminal portion (amino acids 5 to 141) of Lck to obtain the Lck-tagged FE, FEL, and the Lck-tagged AE, AEL, respectively, as described previously [26,27]. The cDNAs encoding these Envs were introduced into pCXN2 to obtain pCXN2FE.D86K, pCXN2FE.T470H, pCXN2AE.T455P, pCXN2R(−)FE, pCXN2R(−)AE, pCXN2FEL, and pCXN2AEL, respectively. The *Fv-4* gene [3] was provided by Ikeda, and an *Fv-4 env* gene fragment amplified by PCR was introduced into pCXN2 to obtain pCXN2Fv4E.

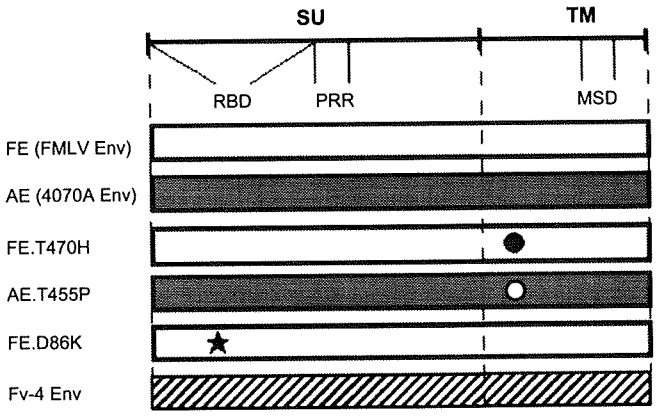

Fig. 1. Structure of MLV Env constructs. FE is the wild-type FMLV Env (indicated by an open box) and AE is the wild-type amphotropic MLV (4070A) Env (indicated by a closed box). FE.T470H is a defective FMLV Env with a point mutation (indicated by a closed circle) in the extracellular domain of TM. AE.T455P is a defective amphotropic MLV Env with a point mutation (indicated by an open circle) in the extracellular domain of TM. FE.D86K is a defective FMLV Env with a point mutation (indicated by a star) in the receptor-binding domain (RBD). Fv-4 Env is indicated by a striped box. PRR represents the proline-rich region in SU and MSD represents the membrane-spanning domain in TM.

2.2. Western blot analysis

Cells were cultured in Dulbecco's modified minimal essential medium supplemented with 10% fetal bovine serum. An MoMLV *gag–pol* producer cell line harboring a lacZ-expressing retroviral vector (MFGnlslacZ), TELCeB6 [28], was provided by Cosset and Takeuchi. For harvesting cellular proteins, cells were plated at a density of 2×10^5 cells per well in 6-well plates, incubated overnight, transfected with 2 μg or indicated amounts of DNAs using Lipofectamine (Invitrogen, Tokyo, Japan), and two days later, were lysed with 0.6 ml of triple-detergent lysis buffer (50 mM Tris-HCl, pH 8.0, 150 mM NaCl, 0.02% sodium azide, 0.1% sodium dodecyl sulfate, 0.5% sodium deoxycholate, 0.1 mg/ml phenylmethylsulfonyl fluoride [PMSF], 1% Triton X-100). For preparing virion proteins, TELCeB6 cells plated at a density of 6×10^5 cells per T25-flask were transfected with 6 μg or indicated amounts of DNAs, and culture supernatants were harvested two days after DNA transfection, filtered through a 0.45-μm-pore-size filter, and centrifuged at 20,600 × *g* for 8 h. The viral pellets from 1 ml of supernatant were lysed with 25 μl of triple-detergent lysis buffer. Each lane was loaded with 10 μl of lysate and Western blot analysis using a polyclonal goat anti-gp70 (MLV SU) antibody (National Cancer Institute, lot 79S000713) was performed as described previously [29].

2.3. Immunoprecipitation analysis

Two days after DNA transfection, cells in a well of 6-well plates were labeled with [35S]redivue Pro-mix (GE Healthcare, Tokyo, Japan) including [35S]methionine and [35S]cysteine for 30 min and were lysed with 0.6 ml of single-detergent lysis buffer (50 mM Tris-HCl, pH 8.0, 150 mM NaCl, 0.02% sodium azide, 0.1 mg/ml PMSF, 1% Triton X-100).